

Spatio-temporal variability of zooplankton standing stock in eastern Arabian Sea inferred from ADCP backscatter measurements

Ranjan Kumar Sahu, P. Amol, D.V. Desai, S.G. Aparna, D. Shankar

October 15, 2024

Abstract

We use acoustic Doppler current profiler (ADCP) backscatter measurements to map the spatio-temporal variation of zooplankton standing stock in the eastern Arabian Sea (EAS). The ADCP moorings were deployed at seven locations on the continental slope off the west coast of India; we use data from October 2017 to December 2023. The 153.3 kHz ADCP uses backscatter from sediments or organisms such as copepods, ctenophores, salps and amphipods greater than 1 cm to calculate current profile. The backscatter is obtained from echo intensity using RSSI conversion factor after doing necessary calibrations. The conversion from backscatter to biomass is based on volumetric zooplankton sampling at the respective locations. Analysis of the data over 24–120 m shows that the backscatter and zooplankton biomass decrease from the upper ocean (215 mg^{-3} biomass contour) to the lower depths. Changes are observed in the seasonal variation of the monthly

¹² climatology of zooplankton standing stock (integral of the biomass over 24–120 m water column)
¹³ as we move to poleward along the slope in EAS. The range of variation of standing stock is lowest
¹⁴ at Kanyakumari, followed by Okha, which lie at the southern and northern boundary of the EAS,
¹⁵ respectively. Complementary variables are used to explain the processes leading to growth or decay
¹⁶ of zooplankton biomass.

₁₇ **1 Introduction**

₁₈ **1.1 Background**

₁₉ Zooplankton plays a vital role in food web of pelagic ecosystem by enabling the hierarchical trans-
₂₀ port of organic matter from primary producers to higher trophic levels impacting the fish population
₂₁ [Ohman and Hirche, 2001] and the carbon pump of the deep ocean [Le Qu et al., 2016]. They are
₂₂ presumably the largest migrating organisms in terms of biomass [Hays, 2003] which occurs in diel
₂₃ vertical migration (DVM). Zooplanktons depend not only on phytoplankton but other environ-
₂₄ mental parameters (e.g. mixed layer depth, insolation, oxygen, thermocline, nutrient availability,
₂₅ chlorophyll concentration and daily primary production). The biological productivity of the ocean
₂₆ is essentially connected with physics and chemistry [Subrahmanyam, 1959, Ryther et al., 1966,
₂₇ Qasim, 1977, Nair, 1970, Banse, 1995, McCreary et al., 2009, Vijith et al., 2016, Amol et al., 2020].
₂₈ The dynamic ocean results in varying physico-chemical properties, leading to bloom and growth of
₂₉ plankton in favourable conditions. The changes are strongly influenced by the seasonal cycle in the
₃₀ North Indian Ocean (NIO; north of 5 °N of Indian Ocean). The eastern boundary of Arabian Sea
₃₁ contains the West India Coastal Current ([Ramamirtham and Murty, 1965, Banse, 1968, Shetye
₃₂ et al., 1990, McCreary Jr et al., 1993, Amol et al., 2014, Vijith et al., 2016, Chaudhuri et al., 2020,
₃₃ WICC]) which reverses seasonally, flowing poleward (equatorward) during November to February
₃₄ (June to September).

₃₅ A direct consequence of this reversal is the seasonal cycle of thermocline, oxycline and thickness
₃₆ of mixed Layer Depth (MLD) induced by upwelling (downwelling) favourable conditions in summer
₃₇ (winter) eastern Arabian Sea (EAS) facilitated further by wind speed and near-surface stratifica-
₃₈ tion. Further, the phytoplankton biomass and chlorophyll concentration changes with the season

39 [Subrahmanyam and Sarma, 1960, Banse, 1968, Lévy et al., 2007, Vijith et al., 2016]. Upwelling in
40 summer monsoon leads to maximum chlorophyll growth in the entire EAS [Banse, 1968, Banse and
41 English, 2000, McCreary et al., 2009, Hood et al., 2017, Shi and Wang, 2022]. During winter mon-
42 soon, the convective mixing induced winter mixed layer [Shetye et al., 1992, Madhupratap et al.,
43 1996b, McCreary Jr et al., 1996, Lévy et al., 2007, Shankar et al., 2016, Vijith et al., 2016, Keerthi
44 et al., 2017, Shi and Wang, 2022] results in winter chlorophyll peak in northern EAS (NEAS) while
45 the downwelling Rossby waves modulate chlorophyll along the southern EAS (SEAS) albeit limited
46 to coast and islands [Amol et al., 2020].

47 The zooplankton grazing peak is instantaneous with no time delay from peak phytoplankton
48 production [Li et al., 2000, Barber et al., 2001], but its population growth lags [Rehim and Imran,
49 2012, Almén and Tamelander, 2020] depending on its gestation period and other limiting aspects.
50 While some studies suggest that the peak timing of zooplankton may not change in parallel with
51 phytoplankton blooms [Winder and Schindler, 2004], others indicate that lag exists between primary
52 production and the transfer of energy to higher trophic levels [Brock and McClain, 1992, Brock
53 et al., 1991]. The conventional zooplankton measurements, where only few snapshot/s of the event
54 is captured gives an incoherent or incomplete understanding in terms of spatio-temporal variation
55 of zooplankton [Ramamurthy, 1965, Piontkovski et al., 1995, Madhupratap et al., 1992, 1996a,
56 Wishner et al., 1998, Kidwai and Amjad, 2000, Barber et al., 2001, Khandagale et al., 2022] as
57 much information is revealed by later studies [Jyothibabu et al., 2010, Vijith et al., 2016, Shankar
58 et al., 2019, Aparna et al., 2022] using high resolution data. Calibrated acoustic instruments such
59 as acoustic Doppler current profiler (ADCP) along with relevant data can be utilised to understand
60 small scale variability [Nair et al., 1999, Edvardsen et al., 2003, Smith and Madhupratap, 2005, Smeti
61 et al., 2015, Kang et al., 2024], the complex interplay between the physico-chemical parameters and

62 ecosystem [Jiang et al., 2007, Potiris et al., 2018, Shankar et al., 2019, Aparna et al., 2022, Nie
63 et al., 2023], the zooplankton migration [Inoue et al., 2016, Ursella et al., 2018, 2021] and their
64 seasonal to annual variation [Jiang et al., 2007, Hobbs et al., 2021, Liu et al., 2022, Aparna et al.,
65 2022].

66 The relationship between backscatter and the abundance & size of zooplankton was described by
67 Greenlaw [1979] wherein it was pointed out that single frequency backscatter can be used to estimate
68 abundance if mean zooplankton size is known. A drastic increase in study temporal and spatial
69 variation of zooplankton biomass using backscatter-proxy came in 1990s by introduction of high
70 frequency echo sounders, with studies [Flagg and Smith, 1989, Wiebe et al., 1990, Batchelder et al.,
71 1995, Greene et al., 1998, Rippeth and Simpson, 1998] methodically showing acoustic backscatter
72 estimated zooplankton biomass. Net sampling augmented ADCP backscatter have been used to
73 study DVM and the spatial and temporal variability of zooplankton biomass in different marine
74 regions, such as the Southwestern Pacific, the Lazarev Sea in Antarctica and the Corsica Channel in
75 the north-western Mediterranean Sea [Cisewski et al., 2010, Hamilton et al., 2013, Smeti et al., 2015,
76 Guerra et al., 2019]. The first such study to exploit the potential of ADCPs in EAS was carried out
77 by Aparna et al. [2022] (A22 from hereon) using ADCP moorings deployed on continental slopes off
78 the Indian west coast. In their work, they showed that the zooplankton standing stock (ZSS) in fact
79 declines during upwelling facilitated increase in phytoplankton biomass. The unusual interaction
80 implies the break down of existing understanding of predator-prey relationship in fundamental level
81 of marine food chain.

82 **1.2 Objective and scope of the manuscript**

83 A network of ADCPs has been installed off the continental slope and shelf on the west coast of
84 India. This ADCPs have enabled a rigorous view of intraseasonal to seasonal scale variability [[Amol](#)
85 [et al., 2014](#), [Chaudhuri et al., 2020](#)] of WICC. In the recent study A22 have used ADCP moorings
86 off Mumbai, Goa and Kollam to explain the temporal variability of zooplankton biomass. The
87 study showed that the zooplankton peaks (and troughs) is not only non-uniform in latitude but
88 also heavily influenced by the oxygen minimum zone, MLD and the seasonal upwelling/downwelling
89 conditions. Stark contrast in the phytoplankton bloom and subsequence growth of zooplankton or
90 the lack thereof was observed in the EAS regimes.

91 We extend the work of A22 by presenting data from four additional moorings in the EAS, show-
92 casing the deviations of seasonal cycle from climatology, and discussing the significant intraseasonal
93 variability of biomass and standing stock revealed by the ADCP data. The paper is organized as
94 follows; datasets and methods employed are described in section 2. Section 3 describes the observed
95 climatology of zooplankton biomass and standing stock. A comparison is drawn to the results of
96 A22. Further, the seasonal cycle of zooplankton biomass and standing stock is discussed with re-
97 lation to the MLD, oxygen, temperature and circulation in determining the biomass is discussed
98 in results section 4. Section 5 delves deeper into the intraseasonal variability with summary and
99 conclusion in section 6.

100 **2 Data and methods**

101 The backscatter data from ADCP and the zooplankton samples collected from the periphery of
102 mooring is described in this section. The backscatter derived from the echo intensity of the seven

103 ADCP mooring deployed on the continental slope off the Indian west coast is the primary data
104 we have use in this manuscript. The moorings details are summarized in [Table 1](#). In situ biomass
105 data from volumetric zooplankton samples are used to validate and correlate with backscatter. The
106 chlorophyll data is obtained from [marine.copernicus.eu](#). In addition, we have used the monthly cli-
107 matology of temperature and salinity [[Chatterjee et al., 2012](#)] and the net primary productivity from
108 MODIS (Moderate Resolution Imaging Spectroradiometer) and VIIRS (Visible Infrared Imaging
109 Radiometer Suite) from global NPP estimates (<http://sites.science.oregonstate.edu/ocean.productivity>).

110 **2.1 ADCP data and backscatter estimation**

111 The ADCPs were deployed on the continental slope off the Indian west coast ([Fig. 1](#)), off Mum-
112 bai, Goa, Kollam and Kanyakumari, and later extended to three more sites to cover the entire
113 EAS basin from Okha (22.26°N) in north to Kanyakumari (6.96°N) in south. The other two
114 ADCPs are Jaigarh at central EAS (CEAS) and Udupi (primarily at SEAS regime) in the transi-
115 tion zone between CEAS & SEAS. The extended moorings were deployed in October 2017, though
116 Kanyakumari had been deployed earlier too. However, only Mumbai, Goa and Kollam were part
117 of the previous backscatter study by A22. The moorings are serviced on yearly basis usually dur-
118 ing October–November or sometime during September–December (depending on ship availability).

119 The ADCPs are of RD Instruments make, upward-looking and operate at 153.3 kHz. While utmost
120 care is taken to position the instrument at ~ 200 m depth, yet for some deployments it's shallow
121 or deeper owing to drift caused by floater buoyancy-anchor weight balance. Data was collected at
122 hourly interval and the bin size was set to 4 m. The echoes at surface to 10% range (~ 20 m) means
123 the data at these depths is rendered useless and is discarded from further use. We have followed
124 the methodology laid down in A22 to derive the backscatter time series from ADCP echo intensity

¹²⁵ data. The gaps up to two days are filled using the grafting method of [Mukhopadhyay et al. \[2017\]](#)
¹²⁶ once the zooplankton biomass time series is constructed.

¹²⁷ 2.2 Zooplankton data and estimation of biomass

¹²⁸ The zooplankton samples were collected in the vicinity (~ 10 km) of ADCP mooring site twice, once
¹²⁹ prior retrieval and again post deployment of moorings so that there is overlap in the ADCP time
¹³⁰ instance and in situ zooplankton samples. The sampling is done at the mooring location during
¹³¹ servicing cruises on board RV Sindhu Sankalp and RV Sindhu Sadhana ([table 2](#)). Multi-plankton
¹³² net (MPN) (100 μm mesh size, 0.5 m^2 mouth area) was used to get samples in the pre-determined
¹³³ depth ranges; water volume filtered was calculated by the product of sampling depth range and the
¹³⁴ mouth area of net. The depth range and timing of sample collection was different throughout the
¹³⁵ MPN hauls (refer [Table 2](#)). From 2020 onward, the depth-range was standardized to the bins of 0
¹³⁶ – 25, 25 – 50, 50 – 75, 75 – 100, 100 – 150 (units are in meters). The backscatter obtained earlier is
¹³⁷ averaged in vertical corresponding to the specific MPN hauls for each site. The backscatter is linear
¹³⁸ regressed with respective biomass to establish their relationship, which has been demonstrated in
¹³⁹ numerous previous studies [[Flagg and Smith, 1989](#), [Heywood et al., 1991](#), [Jiang et al., 2007](#), [Aparna](#)
¹⁴⁰ [et al., 2022](#)].

¹⁴¹ 2.2.1 Biomass time series and estimation of standing stock

¹⁴² The zooplankton biomass time series ([Fig. 3](#)) is created from the above derived linear relationship.
¹⁴³ The standing stock is determined by taking the depth integral of biomass over the water column.
¹⁴⁴ To maintain the consistency of standing stock estimation, only those deployments that doesn't lack
¹⁴⁵ data at any depth in the entire range of 24–120 m are considered for analysis as in A22. The lack of

¹⁴⁶ data in the above mentioned depth range is due to deviation in positioning of ADCP sensor in the
¹⁴⁷ water column. A swift alteration in bathymetry along the continental slope implies that the mooring
¹⁴⁸ might anchor at a different depth than planned, hence a change in the predicted position of ADCP.
¹⁴⁹ This leads to gap in data at few mooring sites for some year. For example, for the northern-most
¹⁵⁰ mooring at Okha, data is not available for the entire upper 120 m depth for the second deployment.
¹⁵¹ Also at Jaigarh, where the surface to ~60m data (in 3rd deployment) and Kollam, where 80 m
¹⁵² and below (in 4th deployment) is unavailable and hence discarded from standing stock estimation.
¹⁵³ There are few deployments where no data or bad data was recorded e.g, at Udupi (4th deployment)
¹⁵⁴ and Kanyakumari (6th deployment).

¹⁵⁵ 2.3 Mixed-layer depth, temperature and oxygen

¹⁵⁶ As we are using a 153.3 kHz ADCP moored at ~ 150 m, the top ~ 10% of data is unusable because
¹⁵⁷ of surface echoes. MLD in EAS is of the order ~ 20 to 40 m during summer monsoon [[Shetye et al., 1990](#), [Shankar et al., 2005](#), [Sreenivas et al., 2008](#)] especially in the SEAS [[Shenoi et al., 2005](#)],
¹⁵⁸ but during winter the MLD in northern NEAS remains deep [[Shankar et al., 2016](#)]. Although it
¹⁵⁹ is possible to use the near-surface ADCP data after due noise correction, it is beyond the scope of
¹⁶⁰ present study. The temperature data is used from [Chatterjee et al. \[2012\]](#), a monthly climatology
¹⁶¹ having 1° spatial resolution. Monthly climatology of oxygen data is obtained from World Ocean
¹⁶² Atlas 2013 [[García et al., 2014](#)] which contains objectively analyzed 1° climatological fields of in
¹⁶³ situ measurements.

165 **2.4 Chlorophyll and net primary productivity data**

166 Previous study based on ADCP data of EAS A22 have used SeaWiFS based chlorophyll data for
167 comparison with climatology of ZSS. The SeaWiFS was at its end of service in 2010, hence we use
168 new chlorophyll product. While the chlorophyll product only captures chlorophyll at surface, the
169 productivity models consists information in depth containing the subsurface chlorophyll maxima.
170 The present study has been conducted using Global Ocean Colour, biogeochemical, L3 data obtained
171 from the [E.U. Copernicus Marine Service Information](#). The daily data is available at a spatial
172 resolution of 4 km.

173 **3 Climatology of zooplankton biomass and standing stock**

174 The high and low productive biomass regime in upper and deeper depths is demarcated using a
175 biomass contour as in A22 who chose 215 mg m^{-3} as such, and it's depth is labeled as D215. How-
176 ever, in the present scenario we've moorings deployed at farther ends of EAS, namely Kanyakumari
177 (at SEAS) and Okha (at NEAS). The choice of biomass contour isn't abrupt; first, it is carefully
178 chosen to accommodate the seasonal variation, as a shift to biomass contour lower than the z215
179 would be unviable as our data is only till 140 m depth. For example in the case of Kollam, the
180 D215 exceeds 140 during few months of 2022 ([Fig. 3](#)). A higher biomass contour would lead to
181 subdued view of the seasonal cycle as in the case of Kanyakumari and Okha where 215 mg m^{-3}
182 biomass contour is often low enough to reach $\sim 20\text{--}30 \text{ m}$ depths ([Fig. 3](#)), hence z175 is chosen here.
183 Second, it allows us to link the seasonal variation of biomass to the physico-chemical properties.
184 Climatology of zooplankton biomass and ZSS is discussed at locations northward starting from
185 southernmost mooring site i.e, Kanyakumari. The time series is discussed briefly in the following

186 subsection. The monthly climatology of biomass and ZSS is computed for all locations having valid
187 data in 24–140 m depth range ([Fig. 4](#)). A comparison is made in later paragraphs with availability
188 of new data.

189 **3.1 Southern EAS**

190 During mid-March off Kanyakumari, the depth of 23 ° C isotherm (henceforth D23) shallows along-
191 with oxycline (marked by 2.1 ml L^{-1} , a higher oxygen contour as it lies outside OMZ core) and
192 a rise in biomass is observed ([Fig. 4 g1](#)). The z175 is shallower from May onward to October
193 and the zooplankton biomass is comparatively higher than rest of the year. D175 deepens starting
194 from October and the relatively high biomass in water column is maintained till late December.
195 However, the deepening of D175 isn't reflected as an increase in ZSS because of low biomass in
196 the entire water column. A gradual increase is seen in the chlorophyll biomass starting from April
197 and the peak is attained in June ([Fig. 4 g2](#)). The ZSS is increased in June, however the growth is
198 minimal. There is almost no seasonal variation in ZSS off Kanyakumari (ZSS std, 0.67 gm m^{-2})
199 as compared to the ZSS variation at the nearest northern mooring site off Kollam (ZSS std, 1.25 gm m^{-2}),
200 where a strong seasonal cycle is observed and the D215 is deeper for any given month.

201 Off Kollam, a higher biomass is present in the larger portion of water column and the D215 is
202 at $\sim 110 \text{ m}$ during Mar–May ([Fig. 4 f1](#)). Starting from March, the D215 begins to shallow with
203 progress in time till August. During this period, a sharp decrease is seen in the D23 ($\sim 80 \text{ m}$ in
204 June to September) while the oxycline (1.7 ml L^{-1} overshoots and reaches $\sim 40 \text{ m}$) ([Fig. 4 f1](#)). A
205 steep rise in chlorophyll biomass is seen off Kollam and its peak is attained in August ([Fig. 4 f2](#)).
206 The ZSS declines in the same period and reaches a minimum when the chlorophyll biomass is at its
207 peak. The chlorophyll biomass decreases rapidly in the following months, while the ZSS increases

208 and a maximum is seen during October. This feature was previously reported by A22, highlighting
209 an imbalance in the interaction between zooplankton and phytoplankton.

210 A similar feature is seen further north, off Udupi which sits at the transition zone of SEAS &
211 CEAS, albeit with a relatively weaker zooplankton biomass. The peak of chlorophyll and minimum
212 of ZSS occurs in September ([Fig. 4 e2](#)) which is one month later than off Kollam. The 2.1 ml L^{-1}
213 oxygen contour overshoots thermocline, however it reaches to a much shallow depth of $\sim 20 \text{ m}$
214 during July to October unlike any other location in our EAS study area. The D215 vaguely follows
215 D23; with the gradual shallowing from March onward reaching $\sim 60 \text{ m}$ in September and a steep
216 decline afterwards till November ([Fig. 4 e1](#)).

217 3.2 Central EAS

218 Off Goa, the D215 seasonal trend is as in A22 and is similar to Udupi since it is entirely restricted
219 by D23 and 1.7 ml L^{-1} oxygen contour that closely follows it. Although we witness an increase in
220 chlorophyll biomass in October, the D215 is restricted to the $\sim 50 \text{ m}$ in this period and the ZSS is
221 at minimum similar to off Udupi (Kollam) during September (August). The ZSS rapidly increases
222 and reaches its maximum in January, sustained till March and then gradually declines. Unlike the
223 previous locations, the biomass off Goa decreases rapidly below the z215 as reported earlier in A22,
224 reaching as low as 60 mg m^{-3} at 130 m during June to September ([Fig. 4 d1](#)).

225 The ZSS off Jaigarh is identical but stronger to that of off Goa, owing to higher biomass above
226 z215 and the comparatively deeper D215 ([Fig. 4 c1](#)). From the ZSS maximum in February ([Fig. 4](#)
227 c2), it steadily decreases and attains a minimum in September, a rapid rise is seen in the following
228 months. What's intriguing is a presence of strong seasonal cycle in ZSS off Jaigarh ($\text{std } 3.24 \text{ gm m}^{-2}$,
229 highest among all locations) although the seasonal variation in chlorophyll biomass ([Fig. 4 c2](#)) is

²³⁰ visibly non-existent (0.05 mg m^{-3} Chl std, lowest among all locations). This is an exact opposite
²³¹ scenario of Kanyakumari, where an insignificant seasonal variation in ZSS (0.67 gm m^{-2} ZSS std)
²³² is seen even though the chlorophyll biomass varies strongly (0.51 mg m^{-3} Chl std).

²³³ Starting from Kollam (Fig. 4 f1) and moving northward to Jaigarh (Fig. 4 c1), we see that the
²³⁴ core of high zooplankton biomass gradually shifts from summer (off Kollam) to winter monsoon (off
²³⁵ Jaigarh), with the transition of upper ocean zooplankton biomass happening along Udupi and Goa.
²³⁶ On the contrary, the chlorophyll biomass tends to have low seasonal range as we move northward
²³⁷ from SEAS, with Jaigarh having the least seasonal variation. This shift along with winter monsoon
²³⁸ facilitated deeper thermocline leads to an even larger impact on ZSS.

²³⁹ 3.3 Northern EAS

²⁴⁰ Further north off Mumbai the D215 is deeper in December to early April, resulting in a higher
²⁴¹ ZSS (Fig. 4 b2). D23 follows D215 and the oxycline follows an erratic pattern, reaching depths
²⁴² > 140 during January to March (Fig. 4 b1); when a higher biomass is observed above z215. The
²⁴³ chlorophyll biomass shows seasonal variation albeit lower than the SEAS counterpart. The ZSS
²⁴⁴ increases rapidly from its minima in October in the following month as the D215 deepens and
²⁴⁵ the maximum occurs in February. The chlorophyll biomass decreases from March and a gradual
²⁴⁶ decrease in ZSS is seen till July, after which the ZSS basically flattens even though the chlorophyll
²⁴⁷ increases.

²⁴⁸ At the northernmost site of EAS i.e, off Okha, a noticeable feature is a much higher oxygen
²⁴⁹ in upper ocean except during summer monsoon, therefore a higher oxygen value is used for the
²⁵⁰ oxycline contour. The biomass above z175 is much weaker (Fig. 4 a1) leading to a relatively lower
²⁵¹ ZSS (Fig. 4 a2) compared to Mumbai. The D175 shallows from February to it's minimum in August.

252 There's two chlorophyll peak off Okha, one in February due to convective mixing induced deepening
253 of MLD [Wiggert et al., 2005, Lévy et al., 2007, Keerthi et al., 2017, Shankar et al., 2016] and the
254 other during August in summer monsoon [Wiggert et al., 2005, Lévy et al., 2007]. The ZSS remains
255 flat in summer monsoon period i.e, June to September, although the chlorophyll biomass increases
256 in this time. Afterwards, ZSS gradually increases and attains its maximum in February same as
257 the chlorophyll biomass. ZSS sustains this maximum till March, declines rapidly in April and then
258 gradually till July.

259 **3.4 Comparison to biomass and ZSS climatology of A22**

260 It is observed that D215 is shallower at all locations and as a result a lower biomass and ZSS as
261 seen in the climatology of the present study (Fig. 5). The difference in D215 is prominent off Goa;
262 while in the previous climatology (Fig. 5 b1) the D215 is deeper and lies along D23, in the present
263 climatological data the D215 is shallower and lies \sim 20–40 m above the D23 during January to
264 April (Fig. 5 b2). A relatively lower biomass is present above z215 year round which reflects in
265 overall lower ZSS of Goa and Mumbai. In the present data, the ZSS maximum off Mumbai occurs
266 in March instead of February (A22), due to a lower ZSS value. The second maximum occurs in
267 August (Fig. 5 d1) and is less pronounced in recent data (Fig. 5 d2). There is dramatic decrease in
268 the minima off Mumbai that occurs in October and ZSS increases rapidly afterwards till February.
269 Off Kollam, higher biomass occurs from May to June in A22, and from May to June and September
270 to November in the present study, with a ZSS minima in August (Fig. 4 c2, d2). The higher ZSS
271 on either side to this minima is less pronounced in A22. This difference in ZSS is clearly seen in the
272 correlation, which is 0.60 off Kollam, while it is 0.94 and 0.98 off Mumbai and Goa, respectively. The
273 correlation reflects ZSS trend similarity, not magnitude deviation over time. In the present study,

²⁷⁴ chlorophyll biomass peaks across all locations in August, revealing a zooplankton-phytoplankton
²⁷⁵ relationship discrepancy off Kollam, consistent with A22 findings.

²⁷⁶ 3.5 Time series of zooplankton biomass

²⁷⁷ A preliminary analysis of the biomass time series in daily and monthly averaged scale shows that
²⁷⁸ the biomass decreases with increasing depth ([Fig. 3](#)) at all the seven locations. Rate of biomass
²⁷⁹ decrease with depth, roughly defined as the difference between mean biomass at 40 m and 104 m
²⁸⁰ depth is highest off Jaigarh and Mumbai as it has higher biomass in upper ocean ([Fig. 6 c,b](#)) and
²⁸¹ lowest off Kanyakumari. This is followed by CEAS locations Goa and Udupi ([Fig. 6 d,e](#)). While the
²⁸² biomass decrease with depth is lower off Kollam from 2017 to 2020, it becomes considerably high
²⁸³ from thereon ([Fig. 6 f](#)). A pattern that develops with lower mean biomass off Okha and off Goa
²⁸⁴ bifurcated by higher mean biomass off Mumbai & Jaigarh; while the lower mean biomass off Udupi
²⁸⁵ and off Kanyakumari is divided by higher mean biomass off Kollam. From standard deviation of
²⁸⁶ biomass it is inferred that the sites with higher biomass tends to have higher variation over time
²⁸⁷ as in the case of Mumbai, Jaigarh and Kollam. The mean, standard deviation of biomass, ZSS
²⁸⁸ and chlorophyll are shown in [Table 3](#). Variation in the monthly average or seasonal cycle over
²⁸⁹ time suggests significant interannual variability. A comparatively weaker decline in zooplankton
²⁹⁰ biomass with respect to depth off Okha ([Fig. 3 a1,a2](#)) at NEAS is agreeing with earlier reported
²⁹¹ data [[Wishner et al., 1998](#), [Madhupratap et al., 2001](#), [Smith and Madhupratap, 2005](#), [Jyothibabu
et al., 2010](#)]. The sites at SEAS, especially off Kanyakumari and 2017 to 2020 off Kollam also have
²⁹³ weaker decrease [[Madhupratap et al., 2001](#), [Jyothibabu et al., 2010](#), [Aparna et al., 2022](#)]. However,
²⁹⁴ post 2020 the decline in biomass with depth off Kollam is high owing to a strong bloom in these
²⁹⁵ years reflected as D215 deepening. During winter monsoon, D175 and D215 is deep throughout

296 EAS, but the occurrence of high biomass is distinct to each regime of EAS. Upper ocean shows
297 considerably high biomass during winter at NEAS, on the contrary at SEAS the upper ocean shows
298 higher biomass during summer monsoon even though the D215 & D175 is shallower during this
299 period.

300 4 Seasonal cycle and variability

301 This section will deal with a discussion on the seasonal cycle and variability of biomass and ZSS in
302 annual and intra-annual scale along the three regimes of EAS.

303 The time series data is incomplete due to instrument issues or incorrect ADCP placement. For
304 example, Okha's second deployment (2019–2020) lacked data for the top 140 meters because the
305 instrument was too deep. This makes it hard to analyze annual cycles in regions with limited data.
306 Therefore, we consider locations other than Okha and Jaigarh for the 40 m biomass in annual scale
307 ([Fig. 7](#)). The ZSS time series is obtained by integrating the biomass over 24–120 m of water column,
308 ([Fig. 8](#)). The biomass is decomposed into distinct period bands spanning days to months. Among
309 these, DVM is the simplest variation, determining zooplankton biomass at a given depth with
310 higher (lower) biomass at night (day). On a longer time scale, annual variability reflects changes
311 over the course of a year often influenced by seasonal cycles like monsoons. Intra-annual variability
312 captures fluctuations that occur between seasons, shorter than a year but longer than a season.
313 Intraseasonal variability is about shifts occurring within a season, typically lasting weeks to months
314 and driven by short-term environmental changes. The strength and contribution of components of
315 variability changes over time and differs between EAS regimes. For instance, in 2019 off Kollam
316 ([Fig. 9](#)), intraseasonal variability was dominated by period $< \sim 30$ days. An increase in biomass
317 during the summer monsoon was due to low-frequency variabilities. However, a sharp decline in

318 August resulted from reduced intra-annual and intraseasonal variability, although a weakly positive
319 annual variability was present.

320 From the linear equation correlating biomass and backscatter, the upper and lower bound of
321 error limits equals to $\sim 14 \text{ mg m}^{-3}$ (Fig. 2). The standard deviation incorporating 99.73 % data
322 i.e., $\pm 3 * \sigma$ of intraseasonal variability is $\pm 40 \text{ mg m}^{-3}$ resulting in its range of 80 mg m^{-3} . The
323 intra-annual (annual) variability also has a range of 80 mg m^{-3} (35 mg m^{-3}). This higher range
324 of variability compared to the error range permits us to infer information reliably.

325 **4.1 SEAS**

326 The annual cycle of biomass off Kanyakumari (Udupi & Kollam) is weak (strong), but it varies
327 in time, for example, off Kollam, the wavelet power is stronger post 2020 (Fig. 7 f). The absence
328 (presence) of ZSS annual cycle off Kanyakumari (off Udupi) is confirmed with wavelet analysis
329 (Fig. 8 g1). A biennial peak is observed in Fourier analysis of ZSS of Kollam agreeing with A22.
330 Along with the annual cycle, we observe presence of semi-annual (~ 180 days) cycle at most locations
331 and together they constitute the seasonal cycle which weakens with depth at SEAS sites.

332 To capture the annual variability, the biomass is filtered with Lanczos filter within period of
333 300 to 400 days (Fig. 10). The annual variability off Kanyakumari (22 mg/m^{-3}) is least among all
334 mooring sites, but Kollam and Udupi show strong annual variability. The variability at intra-annual
335 (100–250 days) band tends to be stronger compared to the annual variability and is strengthened
336 during late summer monsoon to transitional monsoon period (Fig. 11) as seen during 2021 (off
337 Udupi) and 2021,2022 (off Kollam). Fourier analysis of the daily biomass time series suggests
338 presence of signals within the intra-annual band off Kanyakumari, e.g, power peaks at ~ 140 and
339 ~ 220 days implying that the variability is strictly restricted to narrow bands within intra-annual

340 band.

341 4.2 CEAS

342 Annual cycle of biomass is comparatively weak off Goa (CEAS) contrary to results of A22 which
343 could be due to shorter time record and low biomass in the recent years as reflected in its ZSS for
344 2018 to early 2020 ([Fig. 8 d1](#)). At Goa and Jaigarh, we see that the semi-annual period dominates
345 seasonal cycle in the same duration ([Fig. 7 d](#)). The dominance of semi-annual cycle is also seen
346 off Kollam. Although the dominance of semi-annual period in seasonal cycle is seen only for some
347 years, a similar feature was discussed for WICC where the intra-annual component dominates the
348 seasonal cycle as we go equatorward with a change in the strength of intra-annual component
349 in time [[Chaudhuri et al., 2020](#)]. The higher intra-annual variability often coincides with shallow
350 D215/D175, for example off Goa during 2020 and 2022, and weak variability coincides with constant
351 depth of D215. This transient nature of variability is due to the spread of energy among all intra-
352 annual periods for 2022 ([Fig. 7](#)) off Goa, while during 2020 the wavelet energy is only present in
353 the semi-annual periods, resulting in a overall weaker intra-annual component.

354 Upward phase propagation in filtered zonal and meridional currents is noted at most mooring
355 sites [[Amol et al., 2014](#)] and in the annual filtered biomass off Goa and southern moorings, we shed
356 a light on this in discussion section using wavelet coherence result.

357 4.3 NEAS

358 Off Mumbai, a strong annual cycle (~ 365 days) dominates the seasonal cycle throughout the time
359 series of biomass (40 m & 104 m [Fig. 7](#)) and ZSS ([Fig. 8](#)). The semi-annual cycle is present at 40
360 m ([Fig. 7](#)) off Mumbai but weakens at 104 m([Fig. 7](#)) resulting in a annual cycle dominated ZSS.

361 Analysis reveals the presence of strong semi-annual cycle off Okha (at 104 m only).

362 The annual variability is strong off Mumbai and Jaigarh (at CEAS & NEAS transition zone)

363 with 3σ range of 41 and 54 mg m^{-3} , respectively, which is highest among EAS regimes. As observed

364 in ocean currents [Amol et al., 2014, Chaudhuri et al., 2020], the annual filtered biomass decreases

365 moderately with depth off Mumbai and the three CEAS sites than off Kollam (Fig. 10). Intra-annual

366 variability of biomass decreases poleward (excluding Kanyakumari) with higher variation seen off

367 Kollam, Udupi and Goa. Off Okha the annual (intra-annual) variability is weaker (comparable) to

368 the variability off Mumbai but with a weak seasonal cycle at upper ocean.

369 5 Intraseasonal variability

370 The intraseasonal band, defined as the variability occurring between periods of few days to 90 days

371 is split into two categories; a high-frequency (period < 30 days) and a low-frequency ($30 <$ period

372 < 90 days) component. The presence of significant variation in the 30-day running mean with

373 recurring bursts are seen in the daily data and in the wavelet analysis of biomass at 40 m and 104

374 m (Fig. 7) as bursts during few months distinctive to each mooring location.

375 The wavelet power at 40 m in low-frequency intraseasonal band peaks during September to

376 December off Mumbai, Jaigarh and Kanyakumari while no such general observation is found in

377 other locations. However, the wavelet power at 104 m in comparison to 40 m suggests a decrease

378 in its strength at respective locations. Lanczos filtered biomass in 30 to 90 day period shows that

379 the intraseasonal variability is strong during August to November off all location (Fig. 12) and is

380 often coherent along much of the EAS slope as seen during 2018. This is in contrast to the WICC

381 intraseasonal band which is strong during winter monsoon at slope [Amol et al., 2014, Chaudhuri

382 et al., 2020] and shelf [Chaudhuri et al., 2021]. The low frequency intraseasonal variability is higher

383 in the upper ocean often limited to the upper 50–70 m, however it can extend to deeper depths (~
384 140 m) for some years e.g, off Jaigarh and Goa during September–November 2018 ([Fig. 12 f](#)). The
385 magnitude of low-frequency component of intraseasonal variability is high as we move equatorward
386 till Kollam much like the intraseasonal currents [[Amol et al., 2014](#), [Chaudhuri et al., 2020, 2021](#)]
387 and declines off Kanyakumari ([Fig. 12 g](#)).

388 The intra-seasonal component is transient in nature and its magnitude is higher than the low
389 frequency variabilities. A strong dependency of zooplankton biomass on the intra-seasonal variation
390 has implication on the sampling of zooplankton using cruises. A servicing cruise along the EAS
391 moorings takes about 12 to 15 days excluding the time to and fro from port to first/last mooring
392 [[Chaudhuri et al., 2020](#), [Aparna et al., 2022](#)]. However, a sampling cruise dedicated to study the
393 spatial variation of zooplankton [[Madhupratap et al., 1992](#), [Smith et al., 1998](#), [Wishner et al., 1998](#),
394 [Kidwai and Amjad, 2000](#)], say for summer monsoon may last a month or more with coarse sampling
395 interval and hence fail to capture the actual biomass within a season for a fair spatial comparison.
396 One such occasion is a dip in zooplankton biomass off Kollam because of intraseasonal variability
397 during August, 2019 ([Fig. 9](#)). The resulting biomass is low even though the primary production in
398 SEAS [[Asha Devi et al., 2010](#), [Jyothibabu et al., 2010](#)] is high and subsequent zooplankton biomass
399 is supposed to be high.

400 The species distribution of phytoplanktons and further zooplanktons in EAS is determined by in-
401 tricate play based on predation, environment, competition [[Raghukumar and Anil, 2003](#)] and hence
402 the size distribution changes [[Madhupratap et al., 1996a](#), [Kidwai and Amjad, 2000](#), [Raghukumar](#)
403 and [Anil, 2003](#), [Smith and Madhupratap, 2005](#), ?], with few species dominating in certain seasons.
404 Habitat patchiness, i.e, irregular distribution of habitats and resources in the deep-sea environment
405 [[Eggleson et al., 1998](#), [Raghukumar and Anil, 2003](#)] contributes to high biodiversity which in turn

406 can have implications for ecosystem dynamics. A high intraseasonal variability in zooplankton
407 biomass suggests that patchiness in the deep-sea environment isn't solely driven by seasonal cycles
408 but also occurs within individual seasons. Further, it can be theorized that patches-specific species
409 will tend to dominate a duration during episodes of intraseasonal bursts which can be verified with
410 carefully planned in situ zooplankton observations.

411 It is to be noted that while the annual cycle dominates the WICC [Amol et al., 2014, Chaudhuri
412 et al., 2020, 2021], contrary to this, the intraseasonal variability that dominates the zooplankton
413 biomass along EAS. On the other hand, the direction of WICC at any given time of the year is un-
414 predictable [Chaudhuri et al., 2020] and advection & entrainment can affect zooplankton biomass,
415 we can expect it to produce such behaviors that can only be resolved with high-frequency intrasea-
416 sonal variations. Strong peaks in intraseasonal band in chlorophyll was evident in Lombscamble
417 periodogram (figure not shown), similar to zooplankton biomass and ZSS, but lacked concrete
418 evidence of direct correlation.

419 6 Discussion

420 6.1 Summary

421 The zooplankton biomass and standing stock across different regions of EAS was examined in this
422 article, highlighting their spatio-temporal trends in the light of physico-chemical parameters using
423 the multi-yearlong ADCP backscatter data from 2017 to 2023.

424 The findings shows notable seasonal variation in zooplankton biomass and ZSS; In SEAS the
425 higher biomass is observed during summer monsoon, while in NEAS the high biomass is observed
426 during winter monsoon with transition of peak biomass happening gradually along CEAS regime

427 (Fig. 4). Off Kollam, a unique double peak in ZSS occurs, one during May to July and another
428 in September to November, suggesting a complex interplay between environmental drivers and
429 zooplankton growth (Fig. 4 f2). Off Kanyakumari, the seasonal variation in ZSS is non-existent
430 even though a dramatic seasonality is seen in primary production. Climatology shows strong decline
431 in biomass w.r.t. depth off Goa, then NEAS sites off Jaigarh, Mumbai and Okha followed by SEAS
432 locations off Udupi, Kollam and Kanyakumari.

433 Seasonal cycle play a crucial role in regulating biomass variability. A strong annual cycle is
434 observed in Northern sites like Mumbai and Jaigarh (Fig. 7), with biomass peaking during winter
435 monsoon months (Fig. 4). However, the Southern and Central regions, particularly off Kollam,
436 exhibit more complex patterns. Off Kollam, the presence of a weak annual cycle and a stronger
437 semi-annual cycle is noted along with a moderately strong biennial cycle. The semi-annual cycle is
438 especially prominent in the Southern EAS, where it contributes significantly to the seasonal biomass
439 changes, while Northern regions is dominated by annual cycle.

440 Intraseasonal variability, particularly in the 30–90 day range, is found to influence zooplankton
441 biomass significantly, especially in the summer monsoon months (Fig. 12), while the high frequency
442 (period $< \sim 30$ days) variability determine changes in smaller temporal scale (Fig. 9). Intraseasonal
443 variability is higher in the Southern EAS, with the Northern regions displaying more stable patterns.
444 The variability in annual scale is weak, while that in intra-annual scale is often comparable to
445 intraseasonal variability. The dependence of biomass on the current is investigated showing linkage
446 in the annual scale as seen off Goa at near-surface depths.

447 **6.2 Physico-chemical drivers of zooplankton biomass**

448 Numerous factors have an impact on the zooplankton population dynamics and growth in the
449 EAS. Throughout the summer monsoon, the Somali current, which flows clockwise in Arabian sea,
450 is essential in moving oxygen-depleted waters creating a perennial oxygen minimum zone (OMZ)
451 [Sarma et al., 2020, Sudheesh et al., 2022]. The net transport of water in upper 500 m of northern
452 Arabian sea is about 5 Sv and a majority of the replaced waters comes from upwelling in the eastern
453 Arabian sea [Shi et al., 1999] during summer monsoon with the high-nutrient water covering \sim 500–
454 700 km from coast [Morrison et al., 1998]. Upwelling supplies nutrients to the surface [Kumar et al.,
455 2000], but it also plays a role in the creation of hypoxic conditions, which can restrict the kinds of
456 zooplankton species that can survive in these waters [Jayakumar et al., 2004]. The upwelling starts
457 in early by February itself off SEAS, but it occurs much later during May farther north along the
458 coast [Banse, 1968, Kumar et al., 2000, Vijith et al., 2016, Sarma et al., 2020] albeit weaker than
459 the southern counterpart. The deepening of MLD in winter due to convective mixing during [Marra
460 and Barber, 2005, Shankar et al., 2016, Shi and Wang, 2022] leads to dilution of zooplankton grazers
461 in water column [Marra and Barber, 2005] and hence longer food chain [Banse, 1995, Barber et al.,
462 2001], explaining the carnivore dominated fisheries in NEAS [Shankar et al., 2019] and planktivore
463 dominated SEAS [Longhurst and Wooster, 1990, Shankar et al., 2019].

464 The southwest monsoon was found to be the most productive period [Kumar et al., 2000]
465 however the observed primary productivity values were lower than predicted primary productivity
466 owing to efficient grazing by mesozooplankton that kept diatom biomass in check instead of high
467 levels of primary productivity as seen in coastal upwelling regions [Barber et al., 2001]. Similar
468 to the zooplankton variability, the inter-annual variability of Chl-a is less in comparison to its
469 seasonal variability [Shi and Wang, 2022] implying the inter-species relationship to be at play in

470 shorter timescale with large and small phytoplankton dominating the SEAS [Shankar et al., 2019].
471 It is inferred that along with the physico-chemical parameters, the biology of ocean determines
472 the zooplankton-phytoplankton relationship and their biomass, respectively. This interdependency
473 of planktons and the physico-chemical drivers shows up as strong intraseasonal and intra-annual
474 variability in zooplankton biomass as demonstrated in section 4.

475 6.3 Current and biomass coherence

476 The annual variability shows that the contribution of this band to the time series of total biomass is
477 very weak. It is low off Kanyakumari (standard deviation 3.64 mg m^{-3}) and Okha (3.73 mg m^{-3}),
478 while it is stronger at rest of the basin, with strongest variability off Jaigarh (9.05 mg m^{-3}). But
479 the variation in chlorophyll biomass off Jaigarh is much lower than that of Kanyakumari. Owing
480 to the above and coherence of current and ZSS, advection as a driver to upwelling and further as
481 one of the cause for zooplankton growth is hypothesized and their relationship is explored. Wavelet
482 coherence shows that the current and biomass have strong coherence off Kanyakumari (2019,2021),
483 Kollam (2019, 2022) during May to late summer monsoon of 2019 with meridional current leading
484 biomass, when the currents are reversing with monsoon (Fig. 13). As we go poleward along the
485 slope, coherence exists but at different depth i.e, off Goa for 2019, the maximum coherence of
486 meridional current with biomass is at 50 to 80 m and again below 110 m. The feature observed
487 in annual filtered biomass off Goa is similar to the alongshore component [Nethery and Shankar,
488 2007], with the core of biomass and alongshore current lying at about 50 m. Further north, off
489 Mumbai a shift in time of maximum coherence is observed occurring in winter monsoon at 80 m
490 and below with zonal current leading biomass. During pre-summer monsoon upwelling sets as early
491 as February in SEAS but only in May farther north along the coast [Banse, 1968] which results

492 in shift in biomass coherence as we go poleward. Off Okha however, present of coherence is seen
493 throughout 2021 from 20 to 150 m with meridional current leading biomass which could be due
494 to a deeper MLD in northern NEAS [Marra and Barber, 2005, Shankar et al., 2016]. This has
495 implications on the nature of zooplankton and fisheries found in regimes of EAS as we'll discuss in
496 the following section.

497 6.4 Decoding the Arabian sea paradox: evolution of our understanding

498 While the zooplankton biomass was expected to have a seasonality, the transient nature of variability
499 also explains why Arabian sea paradox was seen as such. In northern Arabian sea, the extended
500 upwelling time leads to a longer and steady primary production, albeit weaker than the southern
501 counterpart [Madhupratap et al., 1996a, Smith and Madhupratap, 2005]. Provided the zooplankton-
502 phytoplankton interaction is based on primary production, this may lead to the zooplankton biomass
503 to be consistent over season or longer i.e, weaker intraseasonal and intra-annual variability, for
504 example off Goa, June 2019 to September 2020, (Figs. 11 and 12) the D215 remains at same
505 depth, and this could be misinterpreted as constancy in zooplankton biomass leading to paradoxical
506 conclusions.

507 Using the continuous data from ADCP backscatter, A22 showed not only there is a seasonality,
508 but zooplankton-phytoplankton relationship can interact unexpectedly by negative zooplankton
509 growth (dip in ZSS) when the phytoplankton bloom occurs during summer monsoon as was the
510 case of Kollam. However, with the present study extending further boundary of EAS in south
511 of Kollam, we come across Kanyakumari which matches with the paradox posited back in 1990s
512 by Madhupratap et al. [1992, 1996a], Smith and Madhupratap [2005] and studies from JGOFS
513 cruise. Although the difference between the former and present paradox is fundamentally distinct,

514 while former raised the question "how does zooplankton sustain it's population/growth in unviable
515 conditions throughout year?", the present question is "why zooplankton doesn't seem to grow
516 in tune with raising phytoplankton productivity during summer monsoon?". The answer to this
517 question may lie in understanding the intricate interactions between phytoplankton, zooplankton,
518 and fish, as well as the influence of monsoon currents on the availability of essential nutrients and
519 rare elements that zooplankton need but cannot obtain from phytoplankton alone. [Shankar et al.,
520 2019] had found that if the upwelling is sufficiently strong, then phytoplankton tend to grow bigger
521 in size and hence fish can compete directly with zooplankton on predation of phytoplankton, thereby
522 limiting the zooplankton growth substantially which we see as a minuscule rise in ZSS (Fig. 4 g2).
523 For similar reasoning, a dip in ZSS is observed in peak summer monsoon off Kollam during August.

524 6.5 Conclusion

525 The results presented in this paper are based on the ADCP backscatter which is suitable for
526 creating long-term time series of zooplankton biomass in open ocean. There are however, certain
527 limitations to this approach. While the variation in depth is captured with in situ samples from
528 MPN, the variation in season is not adequately addressed owing to the limitation of months when
529 ADCP servicing cruises are undertaken. The west coast cruises for ADCP servicing are planned
530 for the monsoon transition months but may start as early as late September till December with
531 few exceptions such as 2022 when it was carried out in March. Since the intraseasonal and intra-
532 annual variability is almost double that of the annual one, the sampling done in particular season
533 for biomass-backscatter comparison isn't sufficient. For a better approach to capture the seasonal
534 variation, more in situ samples are needed from the less explored seasons.

535 While we are able to infer the biomass information, any information regarding the size distribu-

tion of zooplankton and their contribution to ZSS is lost. In western Arabian sea, microzooplankton dominated the grazing processes by consuming approximately 71 % of the primary production [Reckermann and Veldhuis, 1997, Marra and Barber, 2005, Landry, 2009]. Mesozooplankton, in turn relied on microzooplankton for about 40 % of their food [Landry, 2009, Hood et al., 2024]. However, the relative grazing importance of micro and mesozooplankton fluctuated seasonally and spatially, affecting the overall impact on phytoplankton biomass in a way that aligns with the theory of grazing control or trophic cascade [Ripple et al., 2016] in the Arabian Sea [Marra and Barber, 2005, Landry, 2009]. To understand the intricate complexities of meso and microzooplankton interaction and their size distribution, multi-frequency, size-resolving backscatter data can be utilised.

7 Declaration of competing interest

The authors declare that they have no known competing financial interests or personal relationships that could have appeared to influence the work reported in this paper.

8 Acknowledgments

The data were collected by xxx with fund provided under xxxx. The mooring programme is supported by INCOIS (Indian National Centre for Ocean Information Services, Hyderabad) and CSIR. We acknowledge the contribution of mooring division and ship cell of CSIR-NIO.

Ranjan Kumar Sahu expresses his acknowledgment to the Council of Scientific and Industrial Research (CSIR) for sponsoring his fellowship. Additionally, he extends his thanks to Ashok Kankonkar for providing the essential data, Rahul Khedekar for his data processing, Roshan D'Souza

556 for his diligent work in biological data analysis. Their contributions were invaluable to the successful
557 completion of this research.

558 **References**

- 559 Anna-Karin Almén and Tobias Tamelander. Temperature-related timing of the spring bloom and match between
560 phytoplankton and zooplankton. *Marine Biology Research*, 16(8-9):674–682, 2020.
- 561 P Amol, D Shankar, V Fernando, A Mukherjee, SG Aparna, R Fernandes, GS Michael, ST Khalap, NP Satelkar,
562 Y Agarvadekar, et al. Observed intraseasonal and seasonal variability of the west india coastal current on the
563 continental slope. *Journal of Earth System Science*, 123(5):1045–1074, 2014.
- 564 P Amol, Suchandan Bemal, D Shankar, V Jain, V Thushara, V Vijith, and PN Vinayachandran. Modulation of
565 chlorophyll concentration by downwelling rossby waves during the winter monsoon in the southeastern arabian
566 sea. *Progress in Oceanography*, 186:102365, 2020.
- 567 SG Aparna, DV Desai, D Shankar, AC Anil, Shrikant Dora, and R Khedekar. Seasonal cycle of zooplankton standing
568 stock inferred from adcp backscatter measurements in the eastern arabian sea. *Progress in Oceanography*, 203:
569 102766, 2022.
- 570 C.R. Asha Devi, R. Jyothibabu, P. Sabu, Josia Jacob, H. Habeebrehman, M.P. Prabhakaran, K.J. Jayalakshmi, and
571 C.T. Achuthankutty. Seasonal variations and trophic ecology of microzooplankton in the southeastern arabian
572 sea. *Continental Shelf Research*, 30(9):1070–1084, 2010. ISSN 0278-4343. doi: <https://doi.org/10.1016/j.csr.2010.02.007>. URL <https://www.sciencedirect.com/science/article/pii/S0278434310000439>.
- 574 K Banse and DC English. Geographical differences in seasonality of czcs-derived phytoplankton pigment in the
575 arabian sea for 1978–1986. *Deep Sea Research Part II: Topical Studies in Oceanography*, 47(7-8):1623–1677, 2000.
- 576 Karl Banse. Hydrography of the arabian sea shelf of india and pakistan and effects on demersal fishes. In *Deep sea*
577 *research and oceanographic Abstracts*, volume 15, pages 45–79. Elsevier, 1968.
- 578 Karl Banse. Zooplankton: pivotal role in the control of ocean production: I. biomass and production. *ICES Journal*
579 *of marine Science*, 52(3-4):265–277, 1995.
- 580 Richard T Barber, John Marra, Robert C Bidigare, Louis A Codispoti, David Halpern, Zackary Johnson, Mikel
581 Latasa, Ralf Goericke, and Sharon L Smith. Primary productivity and its regulation in the arabian sea during
582 1995. *Deep Sea Res. Part 2 Top. Stud. Oceanogr.*, 48(6-7):1127–1172, jan 2001.
- 583 H. P. Batchelder, J. R. VanKeuren, R. D. Vaillancourt, and E. Swift. Spatial and temporal distributions of acoustically
584 estimated zooplankton biomass near the marine light-mixed layers station (59°30'n, 21°00'w) in the north atlantic
585 in may 1991. *Journal of Geophysical Research: Oceans*, 100:6549–6563, 1995. doi: 10.1029/94jc00981.

- 586 John C Brock and Charles R McClain. Interannual variability in phytoplankton blooms observed in the northwestern
587 arabian sea during the southwest monsoon. *Journal of Geophysical Research: Oceans*, 97(C1):733–750, 1992.
- 588 John C Brock, Charles R McClain, Mark E Luther, and William W Hay. The phytoplankton bloom in the north-
589 western arabian sea during the southwest monsoon of 1979. *Journal of Geophysical Research: Oceans*, 96(C11):
590 20623–20642, 1991.
- 591 Abhisek Chatterjee, D Shankar, SSC Shenoi, GV Reddy, GS Michael, M Ravichandran, VV Gopalkrishna,
592 EP Rama Rao, TVS Udaya Bhaskar, and VN Sanjeevan. A new atlas of temperature and salinity for the north
593 indian ocean. *Journal of Earth System Science*, 121:559–593, 2012.
- 594 Anya Chaudhuri, D Shankar, SG Aparna, P Amol, V Fernando, A Kankonkar, GS Michael, NP Satelkar, ST Khalap,
595 AP Tari, et al. Observed variability of the west india coastal current on the continental slope from 2009–2018.
596 *Journal of Earth System Science*, 129(1):57, 2020.
- 597 Anya Chaudhuri, P Amol, D Shankar, S Mukhopadhyay, SG Aparna, V Fernando, and A Kankonkar. Observed
598 variability of the west india coastal current on the continental shelf from 2010–2017. *Journal of Earth System
599 Science*, 130:1–21, 2021.
- 600 Boris Cisewski, Volker H Strass, Monika Rhein, and Sören Krägesky. Seasonal variation of diel vertical migration
601 of zooplankton from adcp backscatter time series data in the lazarev sea, antarctica. *Deep Sea Research Part I:
602 Oceanographic Research Papers*, 57(1):78–94, 2010.
- 603 Kent L Deines. Backscatter estimation using broadband acoustic doppler current profilers. In *Proceedings of the
604 IEEE Sixth Working Conference on Current Measurement (Cat. No. 99CH36331)*, pages 249–253. IEEE, 1999.
- 605 A Edvardsen, D Slagstad, KS Tande, and P Jaccard. Assessing zooplankton advection in the barents sea using
606 underway measurements and modelling. *Fisheries Oceanography*, 12(2):61–74, 2003.
- 607 David B Eggleston, Lisa L Etherington, and Ward E Elis. Organism response to habitat patchiness: species and
608 habitat-dependent recruitment of decapod crustaceans. *Journal of experimental marine biology and ecology*, 223
609 (1):111–132, 1998.
- 610 Charles N Flagg and Sharon L Smith. On the use of the acoustic doppler current profiler to measure zooplankton
611 abundance. *Deep Sea Research Part A. Oceanographic Research Papers*, 36(3):455–474, 1989.
- 612 H. E. García, R. A. Locarnini, T. P. Boyer, J. I. Antonov, A. V. Mishonov, O. K. Baranova, M. M. Zweng, J. R.
613 Reagan, and D. R. Johnson. Dissolved oxygen, apparent oxygen utilization, and oxygen saturation. *NOAA Atlas
614 NESDIS 75*, 3, 2014.
- 615 Charles H Greene, Peter H Wiebe, Chris Pelkie, Mark C Benfield, and Jacqueline M Popp. Three-dimensional
616 acoustic visualization of zooplankton patchiness. *Deep Sea Research Part II: Topical Studies in Oceanography*, 45
617 (7):1201–1217, 1998.

- 618 Charles F Greenlaw. Acoustical estimation of zooplankton populations 1. *Limnology and Oceanography*, 24(2):
619 226–242, 1979.
- 620 Davide Guerra, Katrin Schroeder, Mireno Borghini, Elisa Camatti, Marco Pansera, Anna Schroeder, Stefania
621 Sparnocchia, and Jacopo Chiggiato. Zooplankton diel vertical migration in the corsica channel (north-western
622 mediterranean sea) detected by a moored acoustic doppler current profiler. *Ocean Science*, 15(3):631–649, 2019.
- 623 James M Hamilton, Kate Collins, and Simon J Prinsenberg. Links between ocean properties, ice cover, and plankton
624 dynamics on interannual time scales in the canadian arctic archipelago. *Journal of Geophysical Research: Oceans*,
625 118(10):5625–5639, 2013.
- 626 Graeme C Hays. A review of the adaptive significance and ecosystem consequences of zooplankton diel vertical
627 migrations. In *Migrations and Dispersal of Marine Organisms: Proceedings of the 37 th European Marine Biology
628 Symposium held in Reykjavík, Iceland, 5–9 August 2002*, pages 163–170. Springer, 2003.
- 629 Karen J Heywood, S Scrope-Howe, and ED Barton. Estimation of zooplankton abundance from shipborne adcp
630 backscatter. *Deep Sea Research Part A. Oceanographic Research Papers*, 38(6):677–691, 1991.
- 631 Laura Hobbs, Neil S Banas, Jonathan H Cohen, Finlo R Cottier, Jørgen Berge, and Øystein Varpe. A marine
632 zooplankton community vertically structured by light across diel to interannual timescales. *Biology Letters*, 17(2):
633 20200810, 2021.
- 634 Raleigh R Hood, Lynnath E Beckley, and Jerry D Wiggert. Biogeochemical and ecological impacts of boundary
635 currents in the indian ocean. *Progress in Oceanography*, 156:290–325, 2017.
- 636 Raleigh R Hood, Victoria J Coles, Jenny A Huggett, Michael R Landry, Marina Levy, James W Moffett, and Timothy
637 Rixen. Nutrient, phytoplankton, and zooplankton variability in the indian ocean. In *The Indian Ocean and its
638 role in the global climate system*, pages 293–327. Elsevier, 2024.
- 639 Ryuichiro Inoue, Minoru Kitamura, and Tetsuichi Fujiki. Diel vertical migration of zooplankton at the s 1 bioge-
640 chemical mooring revealed from acoustic backscattering strength. *Journal of Geophysical Research: Oceans*, 121
641 (2):1031–1050, 2016.
- 642 D. A. Jayakumar, Christopher A. Francis, S.W.A. Naqvi, and Bess B. Ward. Diversity of nitrite reductase genes
643 (nirs) in the denitrifying water column of the coastal arabian sea. *Aquatic Microbial Ecology*, 2004. doi: 10.3354/
644 ame034069.
- 645 Songnian Jiang, Tommy D Dickey, Deborah K Steinberg, and Laurence P Madin. Temporal variability of zooplankton
646 biomass from adcp backscatter time series data at the bermuda testbed mooring site. *Deep Sea Research Part I:
647 Oceanographic Research Papers*, 54(4):608–636, 2007.
- 648 R Jyothibabu, NV Madhu, H Habeebrehman, KV Jayalakshmy, KKC Nair, and CT Achuthankutty. Re-evaluation
649 of ‘paradox of mesozooplankton’ in the eastern arabian sea based on ship and satellite observations. *Journal of
650 Marine Systems*, 81(3):235–251, 2010.

- 651 Myounghee Kang, Sunyoung Oh, Wooseok Oh, Dong-Jin Kang, SungHyun Nam, and Kyounghoon Lee. Acoustic
652 characterization of fish and macroplankton communities in the seychelles-chagos thermocline ridge of the southwest
653 indian ocean. *Deep Sea Research Part II: Topical Studies in Oceanography*, 213:105356, 2024.
- 654 Madhavan Girijakumari Keerthi, Matthieu Lengaigne, Marina Levy, Jerome Vialard, Vallivattathillam Parvathi,
655 Clément de Boyer Montégut, Christian Ethé, Olivier Aumont, Iyyappan Suresh, Valiya Parambil Akhil, et al.
656 Physical control of interannual variations of the winter chlorophyll bloom in the northern arabian sea. *Biogeosciences*,
657 14(15):3615–3632, 2017.
- 658 Punam A Khandagale, Vaibhav D Mhatre, and Sujitha Thomas. Seasonal and spatial variability of zooplankton
659 diversity in north eastern arabian sea along the maharashtra coast. *Journal of the Marine Biological Association
660 of India*, 64(1):25–32, 2022.
- 661 S Kidwai and S Amjad. Zooplankton: pre-southwest and northeast monsoons of 1993 to 1994, from the north arabian
662 sea. *Mar. Biol.*, 136(3):561–571, apr 2000.
- 663 S. Prasanna Kumar, M. Madhupratap, M. Dileep Kumar, Mangesh Gauns, P.M. Muraleedharan, V. V. S. S. Sarma,
664 and Sílvia Naves de Souza. Physical control of primary productivity on a seasonal scale in central and eastern
665 arabian sea. *Journal of Earth System Science*, 2000. doi: 10.1007/bf02708331.
- 666 Michael R Landry. Grazing processes and secondary production in the arabian sea: A simple food web synthesis
667 with measurement constraints. In *Indian Ocean Biogeochemical Processes and Ecological Variability*, Geophysical
668 monograph, pages 133–146. American Geophysical Union, Washington, D. C., 2009.
- 669 Corinne Le Qu, Robbie M Andrew, Josep G Canadell, Stephen Sitch, Jan Ivar Korsbakken, Glen P Peters, Andrew C
670 Manning, Thomas A Boden, Pieter P Tans, Richard A Houghton, et al. Global carbon budget 2016. *Earth System
671 Science Data*, 8(2):605–649, 2016.
- 672 Marina Lévy, D Shankar, J-M André, SSC Shenoi, Fabien Durand, and Clément de Boyer Montégut. Basin-wide
673 seasonal evolution of the indian ocean's phytoplankton blooms. *Journal of Geophysical Research: Oceans*, 112
674 (C12), 2007.
- 675 M Li, A Gargett, and K Denman. What determines seasonal and interannual variability of phytoplankton and
676 zooplankton in strongly estuarine systems? *Estuarine, Coastal and Shelf Science*, 50(4):467–488, 2000.
- 677 Yanliang Liu, Jingsong Guo, Yuhuan Xue, Chalermrat Sangmanee, Huiwu Wang, Chang Zhao, Somkiat Khokiat-
678 tiwong, and Weidong Yu. Seasonal variation in diel vertical migration of zooplankton and micronekton in the
679 andaman sea observed by a moored adcp. *Deep Sea Research Part I: Oceanographic Research Papers*, 179:103663,
680 2022.
- 681 Alan R Longhurst and Warren S Wooster. Abundance of oil sardine (*sardinella longiceps*) and upwelling on the
682 southwest coast of india. *Can. J. Fish. Aquat. Sci.*, 47(12):2407–2419, dec 1990.
- 683 M Madhupratap, P Haridas, Neelam Ramaiah, and CT Achuthankutty. Zooplankton of the southwest coast of india:
684 abundance, composition, temporal and spatial variability in 1987. 1992.

- 685 M Madhupratap, TC Gopalakrishnan, P Haridas, KKC Nair, PN Aravindakshan, G Padmavati, and Shiney Paul.
686 Lack of seasonal and geographic variation in mesozooplankton biomass in the arabian sea and its structure in the
687 mixed layer. *Current science. Bangalore*, 71(11):863–868, 1996a.
- 688 M Madhupratap, S Prasanna Kumar, PMA Bhattathiri, M Dileep Kumar, S Raghukumar, KKC Nair, and N Rama-
689 iah. Mechanism of the biological response to winter cooling in the northeastern arabian sea. *Nature*, 384(6609):
690 549–552, 1996b.
- 691 M Madhupratap, TC Gopalakrishnan, P Haridas, and KKC Nair. Mesozooplankton biomass, composition and
692 distribution in the arabian sea during the fall intermonsoon: implications of oxygen gradients. *Deep Sea Research*
693 *Part II: Topical Studies in Oceanography*, 48(6-7):1345–1368, 2001.
- 694 John Marra and Richard T. Barber. Primary productivity in the arabian sea: A synthesis of jgofs data. *Progress*
695 *in Oceanography*, 65(2):159–175, 2005. ISSN 0079-6611. doi: <https://doi.org/10.1016/j.pocean.2005.03.004>. URL
696 <https://www.sciencedirect.com/science/article/pii/S007966110500042X>. The Arabian Sea of the 1990s: New
697 Biogeochemical Understanding.
- 698 JP McCreary, Raghu Murtugudde, Jerome Vialard, PN Vinayachandran, Jerry D Wiggert, Raleigh R Hood,
699 D Shankar, and S Shetye. Biophysical processes in the indian ocean. *Indian Ocean biogeochemical processes*
700 and ecological variability
- 701 Julian P McCreary Jr, Pijush K Kundu, and Robert L Molinari. A numerical investigation of dynamics, thermodynamics and mixed-layer processes in the indian ocean. *Progress in Oceanography*, 31(3):181–244, 1993.
- 702 Julian P McCreary Jr, Kevin E Kohler, Raleigh R Hood, and Donald B Olson. A four-component ecosystem model
703 of biological activity in the arabian sea. *Progress in Oceanography*, 37(3-4):193–240, 1996.
- 704 John M Morrison, LA Codispoti, S Gaurin, Burton Jones, V Manghnani, and Z Zheng. Seasonal variation of
705 hydrographic and nutrient fields during the us jgofs arabian sea process study. *Deep Sea Research Part II: Topical*
706 *Studies in Oceanography*, 45(10-11):2053–2101, 1998.
- 707 S Mukhopadhyay, D Shankar, S G Aparna, and A Mukherjee. Observations of the sub-inertial, near-surface east
708 india coastal current. *Cont. Shelf Res.*, 148:159–177, September 2017.
- 709 KKC Nair, M Madhupratap, TC Gopalakrishnan, P Haridas, and Mangesh Gauns. The arabian sea: physical
710 environment, zooplankton and myctophid abundance. 1999.
- 711 PV Nair. Primary productivity in the indian seas. *CMFRI Bulletin*, 22:1–63, 1970.
- 712 D Nethery and D Shankar. Vertical propagation of baroclinic kelvin waves along the west coast of india. *J. Earth*
713 *Syst. Sci.*, 116(4):331–339, aug 2007.
- 714 Lingyun Nie, Jianchao Li, Hao Wu, Wenchoao Zhang, Yongjun Tian, Yang Liu, Peng Sun, Zhenjiang Ye, Shuyang
715 Ma, and Qinfeng Gao. The influence of ocean processes on fine-scale changes in the yellow sea cold water mass
716 boundary area structure based on acoustic observations. *Remote Sensing*, 15(17):4272, 2023.

- 718 MD Ohman and H-J Hirche. Density-dependent mortality in an oceanic copepod population. *Nature*, 412(6847):
719 638–641, 2001.
- 720 SA Piontkovski, R Williams, and TA Melnik. Spatial heterogeneity, biomass and size structure of plankton of the
721 indian ocean: some general trends. *Marine ecology progress series*, pages 219–227, 1995.
- 722 Emmanuel Potiris, Constantin Frangoulis, Alkiviadis Kalampokis, Manolis Ntoumas, Manos Pettas, George Peti-
723 hakis, and Vassilis Zervakis. Acoustic doppler current profiler observations of migration patterns of zooplankton
724 in the cretan sea. *Ocean Science*, 14(4):783–800, 2018.
- 725 SZ Qasim. Biological productivity of the indian ocean. 1977.
- 726 Seshagiri Raghukumar and AC Anil. Marine biodiversity and ecosystem functioning: A perspective. *Current Science*,
727 84(7):884–892, 2003.
- 728 CP Ramamirtham and AVS Murty. Hydrography of the west coast of india during the pre-monsoon period of the
729 year 1962—part 2: in and offshore waters of the konkan and malabar coasts. *Journal of the Marine Biological
730 Association of India*, 7(1):150–168, 1965.
- 731 S Ramamurthy. Studies on the plankton of the north kanara coast in relation to the pelagic fishery. *Journal of
732 Marine Biological Association of India*, 7(1):127–149, 1965.
- 733 M Reckermann and M J W Veldhuis. Trophic interactions between picophytoplankton and micro- and nanozoo-
734 plankton in the western arabian sea during the NE monsoon 1993. *Aquat. Microb. Ecol.*, 12:263–273, 1997.
- 735 Mehbuba Rehim and Mudassar Imran. Dynamical analysis of a delay model of phytoplankton–zooplankton interac-
736 tion. *Applied Mathematical Modelling*, 36(2):638–647, 2012.
- 737 T. P. Rippeth and J. H. Simpson. Diurnal signals in vertical motions on the hebridean shelf. *Limnology and
738 Oceanography*, 43:1690–1696, 1998. doi: 10.4319/lo.1998.43.7.1690.
- 739 William J Ripple, James A Estes, Oswald J Schmitz, Vanessa Constant, Matthew J Kaylor, Adam Lenz, Jennifer L
740 Motley, Katharine E Self, David S Taylor, and Christopher Wolf. What is a trophic cascade? *Trends Ecol. Evol.*,
741 31(11):842–849, November 2016.
- 742 John H Ryther, John R Hall, Allan K Pease, Andrew Bakun, and Mark M Jones. Primary organic production in
743 relation to the chemistry and hydrography of the western indian ocean 1. *Limnology and Oceanography*, 11(3):
744 371–380, 1966.
- 745 VVSS Sarma, TVS Udaya Bhaskar, J Pavan Kumar, and Kunal Chakraborty. Potential mechanisms responsible for
746 occurrence of core oxygen minimum zone in the north-eastern arabian sea. *Deep Sea Research Part I: Oceano-
747 graphic Research Papers*, 165:103393, 2020.
- 748 D Shankar, SSC Shenoi, RK Nayak, PN Vinayachandran, G Nampoothiri, AM Almeida, GS Michael, MR Ramesh
749 Kumar, D Sundar, and OP Sreejith. Hydrography of the eastern arabian sea during summer monsoon 2002.
750 *Journal of earth system science*, 114:459–474, 2005.

- 751 D Shankar, R Remya, PN Vinayachandran, Abhisek Chatterjee, and Ambica Behera. Inhibition of mixed-layer
752 deepening during winter in the northeastern arabian sea by the west india coastal current. *Climate Dynamics*,
753 47:1049–1072, 2016.
- 754 D Shankar, R Remya, AC Anil, and V Vijith. Role of physical processes in determining the nature of fisheries in the
755 eastern arabian sea. *Progress in Oceanography*, 172:124–158, 2019.
- 756 SSC Shenoi, D Shankar, GS Michael, J Kurian, KK Varma, MR Ramesh Kumar, AM Almeida, AS Unnikrishnan,
757 W Fernandes, N Barreto, et al. Hydrography and water masses in the southeastern arabian sea during march–june
758 2003. *Journal of earth system science*, 114:475–491, 2005.
- 759 SR Shetye, AD Gouveia, SSC Shenoi, D Sundar, GS Michael, AM Almeida, and K Santanam. Hydrography and
760 circulation off the west coast of india during the southwest monsoon 1987. 1990.
- 761 SR Shetye, AD Gouveia, and SSC Shenoi. Does winter cooling lead to the subsurface salinity minimum off saurashtra,
762 india? *Oceanography of the Indian Ocean*, pages 617–625, 1992.
- 763 Wei Shi and Menghua Wang. Phytoplankton biomass dynamics in the arabian sea from viirs observations. *Journal
764 of Marine Systems*, 227:103670, 2022.
- 765 Wei Shi, John M Morrison, Emanuele Böhm, and Vijayakumar Manghnani. Remotely sensed features in the us jgofs
766 arabian sea process study. *Deep Sea Research Part II: Topical Studies in Oceanography*, 46(8-9):1551–1575, 1999.
- 767 Houssem Smeti, Marc Pagano, Christophe Menkes, Anne Lebourges-Dhaussy, Brian PV Hunt, Valerie Allain, Martine
768 Rodier, Florian De Boissieu, Elodie Kestenare, and Cherif Sammari. Spatial and temporal variability of zooplank-
769 ton off n ew c aledonia (s outhwestern p acific) from acoustics and net measurements. *Journal of Geophysical
770 Research: Oceans*, 120(4):2676–2700, 2015.
- 771 Sharon Smith, Michael Roman, Irina Prusova, Karen Wishner, Marcia Gowing, LA Codispoti, Richard Barber, John
772 Marra, and Charles Flagg. Seasonal response of zooplankton to monsoonal reversals in the arabian sea. *Deep Sea
773 Research Part II: Topical Studies in Oceanography*, 45(10-11):2369–2403, 1998.
- 774 SL Smith and M Madhupratap. Mesozooplankton of the arabian sea: patterns influenced by seasons, upwelling, and
775 oxygen concentrations. *Progress in Oceanography*, 65(2-4):214–239, 2005.
- 776 Patnaik Sreenivas, KVKRK Patnaik, and KVSR Prasad. Monthly variability of mixed layer over arabian sea using
777 argo data. *Marine Geodesy*, 31(1):17–38, 2008.
- 778 R Subrahmanyam. Studies on the phytoplankton of the west coast of india: Part ii. physical and chemical factors
779 influencing the production of phytoplankton, with remarks on the cycle of nutrients and on the relationship of
780 the phosphate-content to fish landings. In *Proceedings/Indian Academy of Sciences*, volume 50, pages 189–252.
781 Springer, 1959.
- 782 R Subrahmanyam and AH Sarma. Studies on the phytoplankton of the west coast of india. part iii. seasonal variation
783 of the phytoplankters and environmental factors. *Indian Journal of Fisheries*, 7(2):307–336, 1960.

- 784 V. Sudheesh, G.V.M. Gupta, Yudhishtir Reddy, Kausar F. Bepari, N.V.H.K. Chari, C.K. Sherin, S.S. Shaju, Ch.V.
785 Ramu, and Anil Kumar Vijayan. Oxygen minimum zone along the eastern arabian sea: Intra-annual varia-
786 tion and dynamics based on ship-borne studies. *Progress in Oceanography*, 201:102742, 2022. ISSN 0079-6611.
787 doi: <https://doi.org/10.1016/j.pocean.2022.102742>. URL <https://www.sciencedirect.com/science/article/pii/S0079661122000040>.
- 788 Laura Ursella, Vanessa Cardin, Mirna Batistić, Rade Garić, and Miroslav Gačić. Evidence of zooplankton vertical
789 migration from continuous southern adriatic buoy current-meter records. *Progress in oceanography*, 167:78–96,
790 2018.
- 791 Laura Ursella, Sara Pensieri, Enric Pallàs-Sanz, Sharon Z Herzka, Roberto Bozzano, Miguel Tenreiro, Vanessa Cardin,
792 Julio Candela, and Julio Sheinbaum. Diel, lunar and seasonal vertical migration in the deep western gulf of mexico
793 evidenced from a long-term data series of acoustic backscatter. *Progress in Oceanography*, 195:102562, 2021.
- 794 V Vijith, PN Vinayachandran, V Thushara, P Amol, D Shankar, and AC Anil. Consequences of inhibition of mixed-
795 layer deepening by the west india coastal current for winter phytoplankton bloom in the northeastern arabian sea.
796 *Journal of Geophysical Research: Oceans*, 121(9):6583–6603, 2016.
- 797 Peter H Wiebe, Charles H Greene, Timothy K Stanton, and Janusz Burczynski. Sound scattering by live zooplankton
798 and micronekton: empirical studies with a dual-beam acoustical system. *The Journal of the Acoustical Society of
799 America*, 88(5):2346–2360, 1990.
- 800 Jerry D Wiggert, RR Hood, Karl Banse, and JC Kindle. Monsoon-driven biogeochemical processes in the arabian
801 sea. *Progress in Oceanography*, 65(2-4):176–213, 2005.
- 802 Monika Winder and Daniel E Schindler. Climatic effects on the phenology of lake processes. *Global change biology*,
803 10(11):1844–1856, 2004.
- 804 Karen F Wishner, Marcia M Gowing, and Celia Gelfman. Mesozooplankton biomass in the upper 1000 m in the
805 arabian sea: overall seasonal and geographic patterns, and relationship to oxygen gradients. *Deep Sea Research
806 Part II: Topical Studies in Oceanography*, 45(10-11):2405–2432, 1998.

Table 1: ADCP deployment details at the locations. The temporal resolution is 1 hour, bin size(vertical resolution) 4 m. All ADCPs are operated at 153.3 kHz. The moorings are at a water column depth of 950–1200 m on the continental slope and are serviced on yearly basis according to ship availability. The 6th column consists of Reference echo intensity (Er) for each beam, while the 7th column contains the corresponding RSSI conversion factor [Deines, 1999].

Station (Position; $^{\circ}$ E, $^{\circ}$ N)	Date		Depth			
	Deployment	Recovery	Ocean	ADCP	Er	Kc
Okha (67.47, 22.26)	01/10/2018	01/12/2019	996	118	37 , 37 , 37 , 36	0.42 , 0.44 , 0.42 , 0.43
	01/12/2019	04/12/2020	1166	312	39 , 36 , 38 , 36	0.42 , 0.44 , 0.42 , 0.43
	04/12/2020	08/03/2022	1021	144	41 , 37 , 38 , 37	0.42 , 0.44 , 0.42 , 0.43
	08/03/2022	01/01/2023	1019	142	37 , 38 , 39 , 36	0.42 , 0.44 , 0.42 , 0.43
Mumbai (69.24, 20.01)	09/11/2017	29/09/2018	1025	150	36 , 34 , 39 , 42	0.40 , 0.40 , 0.40 , 0.40
	29/09/2018	29/11/2019	1122	125	35 , 36 , 39 , 42	0.40 , 0.40 , 0.40 , 0.40
	29/11/2019	02/12/2020	1143	164	37 , 34 , 39 , 43	0.40 , 0.40 , 0.40 , 0.40
	02/12/2020	06/03/2022	1125	142	36 , 34 , 39 , 42	0.40 , 0.40 , 0.40 , 0.40
	07/03/2022	02/01/2023	1103	158	37 , 34 , 40 , 43	0.40 , 0.40 , 0.40 , 0.40
Jaigarh (71.12, 17.53)	27/10/2017	27/09/2018	1039	198	32 , 35 , 33 , 32	0.45 , 0.45 , 0.45 , 0.45
	27/09/2018	30/10/2019	1032	164	32 , 35 , 33 , 31	0.45 , 0.45 , 0.45 , 0.45
	03/11/2019	30/11/2020	1142	264	32 , 36 , 33 , 32	0.45 , 0.45 , 0.45 , 0.45
	30/11/2020	05/03/2022	1099	119	33 , 36 , 34 , 32	0.45 , 0.45 , 0.45 , 0.45
Goa (72.74, 15.17)	03/10/2017	25/09/2018	1000	174	35 , 37 , 34 , 35	0.44 , 0.44 , 0.40 , 0.41
	25/09/2018	16/10/2019	969	145	38 , 36 , 36 , 34	0.44 , 0.44 , 0.40 , 0.41
	16/10/2019	29/11/2020	966	143	44 , 38 , 36 , 43	0.44 , 0.44 , 0.40 , 0.41
	29/11/2020	03/03/2022	985	157	35 , 40 , 35 , 38	0.44 , 0.44 , 0.40 , 0.41
	03/03/2022	05/01/2023	984	159	35 , 38 , 35 , 34	0.44 , 0.44 , 0.40 , 0.41
Udupi (74.04, 12.5)	05/10/2017	06/10/2018	1028	176	44 , 46 , 29 , 35	0.45 , 0.45 , 0.45 , 0.45
	06/10/2018	18/10/2019	1027	179	32 , 38 , 30 , 36	0.45 , 0.45 , 0.45 , 0.45
	18/10/2019	11/12/2020	1018	168	33 , 37 , 31 , 38	0.45 , 0.45 , 0.45 , 0.45
	11/03/2022	06/01/2023	1036	155	31 , 32 , 32 , 33	0.45 , 0.45 , 0.45 , 0.45
Kollam (75.44, 9.05)	07/10/2017	08/10/2018	1174	200	43 , 55 , 45 , 43	0.49 , 0.50 , 0.49 , 0.50
	08/10/2018	20/10/2019	1160	123	49 , 62 , 46 , 46	0.49 , 0.50 , 0.49 , 0.50
	20/10/2019	13/12/2020	1209	176	52 , 61 , 54 , 55	0.49 , 0.50 , 0.49 , 0.50
	13/12/2020	13/03/2022	1129	91	49 , 51 , 46 , 47	0.49 , 0.50 , 0.49 , 0.50
	13/03/2022	08/01/2023	1149	164	41 , 48 , 43 , 41	0.49 , 0.50 , 0.49 , 0.50
Kanyakumari (77.39, 6.96)	16/11/2016	08/10/2017	1096	252	37 , 36 , 37 , 37	0.42 , 0.44 , 0.42 , 0.43
	08/10/2017	10/10/2018	1055	181	32 , 34 , 38 , 35	0.45 , 0.45 , 0.45 , 0.45
	10/10/2018	22/10/2019	1075	180	36 , 34 , 39 , 36	0.45 , 0.45 , 0.45 , 0.45
	22/10/2019	14/12/2020	1060	167	33 , 35 , 36 , 35	0.45 , 0.45 , 0.45 , 0.45
	14/12/2020	14/03/2022	1184	287	34 , 36 , 36 , 35	0.45 , 0.45 , 0.45 , 0.45

Table 2:

Volumetric samples of zooplankton of various stations. The sampling depth range is standardised for later years for bin range of 0–25m, 25–50m, 50–75m, 75–100m, 100–150m. The abbreviations are in the following manner: Okha (O), Mumbai (M), Jaigarh (J), Goa (G), Udupi (U), Kollam (K), Kanyakumari (KK); The number tags corresponds to particular cruise of a station.

Sample number	Tag	Lat($^{\circ}$ N)	Lon($^{\circ}$ E)	Date	Time (IST)	Sampling depth range (m)
1-3	G1	15.18	72.79	25 Sep 18	452	50–25, 100–50, 150–100
4-6	G2	15.16	72.71	25 Sep 18	2108	50–25, 100–50, 150–100
7-10	G2	15.16	72.71	25 Sep 18	2137	40–20, 60–40, 80–60, 100–80
11-14	J1			26 Sep 18	2000	40–20, 60–40, 80–60, 100–80
15-17	J2			27 Sep 18	2000	50–25, 100–50, 150–100
18-21	J2			27 Sep 18	2100	40–20, 60–40, 80–60, 100–80
22-25	M1	20	69.19	28 Sep 18	2135	40–20, 60–40, 80–60, 100–80
26-27	M1	20	69.19	28 Sep 18	2205	50–25, 100–50
28-29	M2	20.01	69.2	29 Sep 18	2035	50–25, 100–50
30-33	M2	20.01	69.2	29 Sep 18	2057	40–20, 60–40, 80–60, 100–80
34-37	U1			5 Oct 18	2000	40–20, 60–40, 80–60, 100–80
38-40	U1			5 Oct 18	2100	50–25, 100–50, 150–100
41-43	U2			6 Oct 18	2000	50–25, 100–50, 150–100
44-47	U2			6 Oct 18	2100	40–20, 60–40, 80–60, 100–80
48-51	K1	9.06	75.42	8 Oct 18	421	40–20, 60–40, 80–60, 100–80
52-54	K1	9.06	75.42	8 Oct 18	449	50–25, 100–50, 150–100
55-56	K2	9.04	75.4	8 Oct 18	2027	50–25, 100–50
57-60	K2	9.04	75.4	8 Oct 18	2045	40–20, 60–40, 80–60, 100–80
61-64	G2	15.16	72.74	16 Oct 19	829	50–25, 75–50, 100–75, 150–100
65-67	G3	15.16	72.74	16 Oct 19	1812	50–25, 75–50, 100–75
68-70	K2	9.02	75.42	20 Oct 19	840	50–25, 75–50, 100–75
71-74	K3	9.04	75.43	20 Oct 19	1934	50–25, 75–50, 100–75, 150–100
75-78	KK1			22 Oct 19	742	50–25, 75–50, 100–75, 150–100
79-82	KK2			22 Oct 19	1925	50–25, 75–50, 100–75, 150–100
83-86	J1			30 Oct 19	324	50–25, 75–50, 100–75, 150–100
87-89	J2			4 Nov 19	946	75–50, 100–75, 150–100
90-92	M2	19.98	69.22	29 Nov 19	1434	50–25, 75–50, 100–75
93-96	M3	20.01	69.23	30 Nov 19	958	50–25, 75–50, 100–75, 150–100
97-100	O1	22.24	67.49	1 Dec 19	937	50–25, 75–50, 100–75, 150–100
101	O2	22.25	67.46	1 Dec 19	1957	150–100
102-105	G3	15.68	73.22	28 Nov 20	930	50–25, 75–50, 100–75, 150–100
105-108	G4	15.32	73.22	29 Nov 20	1558	50–25, 75–50, 100–75, 150–100
108-110	J2	17.85	71.21	30 Nov 20	1458	75–50, 100–75, 150–100
111-114	J3	17.91	71.21	1 Dec 20	1052	50–25, 75–50, 100–75, 150–100
115-118	M4	20.03	69.38	2 Dec 20	2016	50–25, 75–50, 100–75, 150–100
119-00	O2	22.41	67.8	4 Dec 20	953	150–100
120-123	O3	22.41	67.79	4 Dec 20	2011	50–25, 75–50, 100–75, 150–100
124-127	K3	9.11	75.72	12 Dec 20	2335	50–25, 75–50, 100–75, 150–100
128-131	K4	9.06	75.74	13 Dec 20	1507	50–25, 75–50, 100–75, 150–100
132-134	KK1	7.62	77.63	14 Dec 20	1226	50–25, 75–50
135-138	KK2	7.62	77.63	14 Dec 20	2047	50–25, 75–50, 100–75, 150–100
139-142	G4	15.32	73.21	3 Mar 22	823	50–25, 75–50, 100–75, 150–100
143-146	G5	15.68	73.21	4 Mar 22	1030	50–25, 75–50, 100–75, 150–100
147-150	M5	19.99	69.23	7 Mar 22	957	50–25, 75–50, 100–75, 150–100
151-154	O3	22.24	67.5	8 Mar 22	806	50–25, 75–50, 100–75, 150–100
155-158	U3	12.5	74.04	12 Mar 22	1156	50–25, 75–50, 100–75, 150–100
159-160	K4	9.04	75.42	13 Mar 22	1027	50–25, 75–50, 100–75
161-164	KK3	6.97	77.4	15 Mar 22	1220	50–25, 75–50, 100–75, 150–100

Table 3:

The mean, standard deviation at 40 and 104 m of zooplankton biomass (mg m^{-3}), standard deviation of ZSS (gm m^{-2}) and chlorophyll (mg m^{-3}) at 7 mooring sites are tabulated along with the standard deviation of components of biomass variability, namely intraseasonal, intra-annual and annual.

	40 m biomass		104 m biomass		decrease with depth (40 m - 104m)	standard deviation				
	Mean	Std	Mean	Std		Chl	ZSS	Intraseasonal	Intra-annual	Annual
Okha	230.42	22.84	151.68	25.58	78.74	0.25	1.93	64.26	63.78	22.38
Mumbai	272.86	34.95	182.24	30.34	90.62	0.13	2.9	70.74	83.52	41.58
Jaigarh	278.45	36.52	182.96	48.89	95.49	0.05	3.24	90.3	87.06	54.3
Goa	235.22	30.34	163.02	36.54	72.2	0.15	2.24	76.38	83.76	38.58
Udupi	247.81	34.37	169.37	38.8	78.43	0.55	2	77.22	100.86	41.64
Kollam	272.56	54.94	198.89	50.08	73.67	0.68	1.25	89.94	95.94	41.82
KanyaKumari	207.07	30.42	167.63	20.89	39.44	0.51	0.67	71.88	52.62	21.84

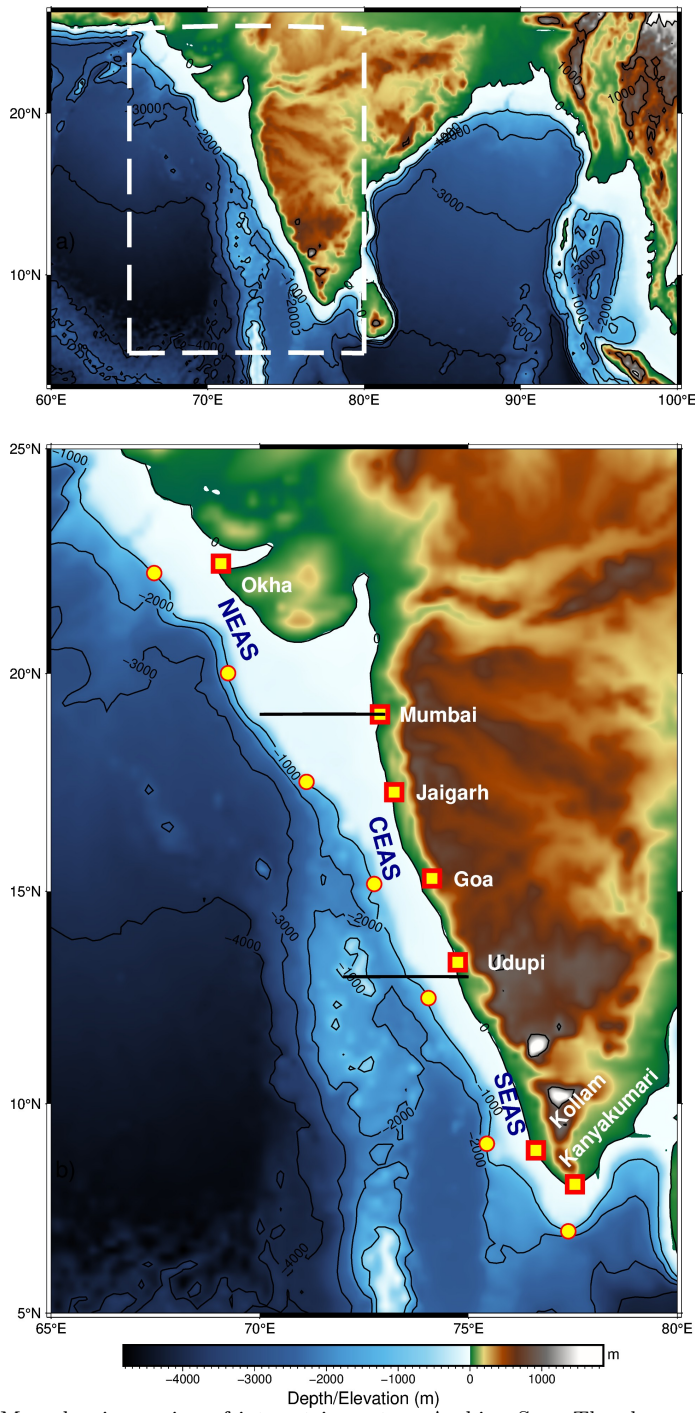


Figure 1: Map showing region of interest in eastern Arabian Sea. The slope moorings are deployed at ~ 1000 m depth as shown in the bathymetry contour. Note the increase in shelf width as we go poleward along the coast. The mooring sites off Okha and Mumbai are in Northern EAS; Jaigarh and Goa in Central EAS while Kollam and Kanyakumari are at Southern EAS. Udupi is situated at the transition zone of Central and Southern EAS.

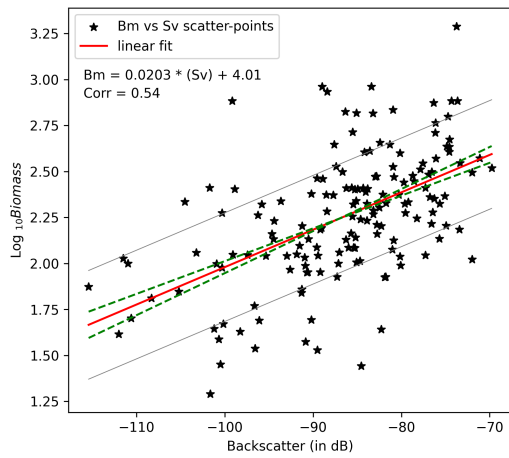


Figure 2: The linear fit line of Biomass (\log_{10} scale) and backscattering strength (in dB). The linear fit line is within the error range of previous result of [Aparna et al., 2022] (contained 67 data points) onto which latest zooplankton volumetric sample data (159 data points) is appended. The regression equation is $y = (0.02 \pm 0.0025) x + (4.0144 \pm 0.2198)$ and correlation value of 0.54. The dashed green lines denote error range of plausible slope and intercept. From the linear equation, the upper and lower bound of error limit leads to an error bar of $\sim 14 \text{ mg m}^{-3}$. The first standard deviation of $\log_{10}(\text{Biomass})$ is ± 0.49 , which results in the backscatter range of 48.58 dB encompassing the entire backscatter range. It signifies the robustness of zooplankton biomass dependency on ADCP measured backscattering strength.

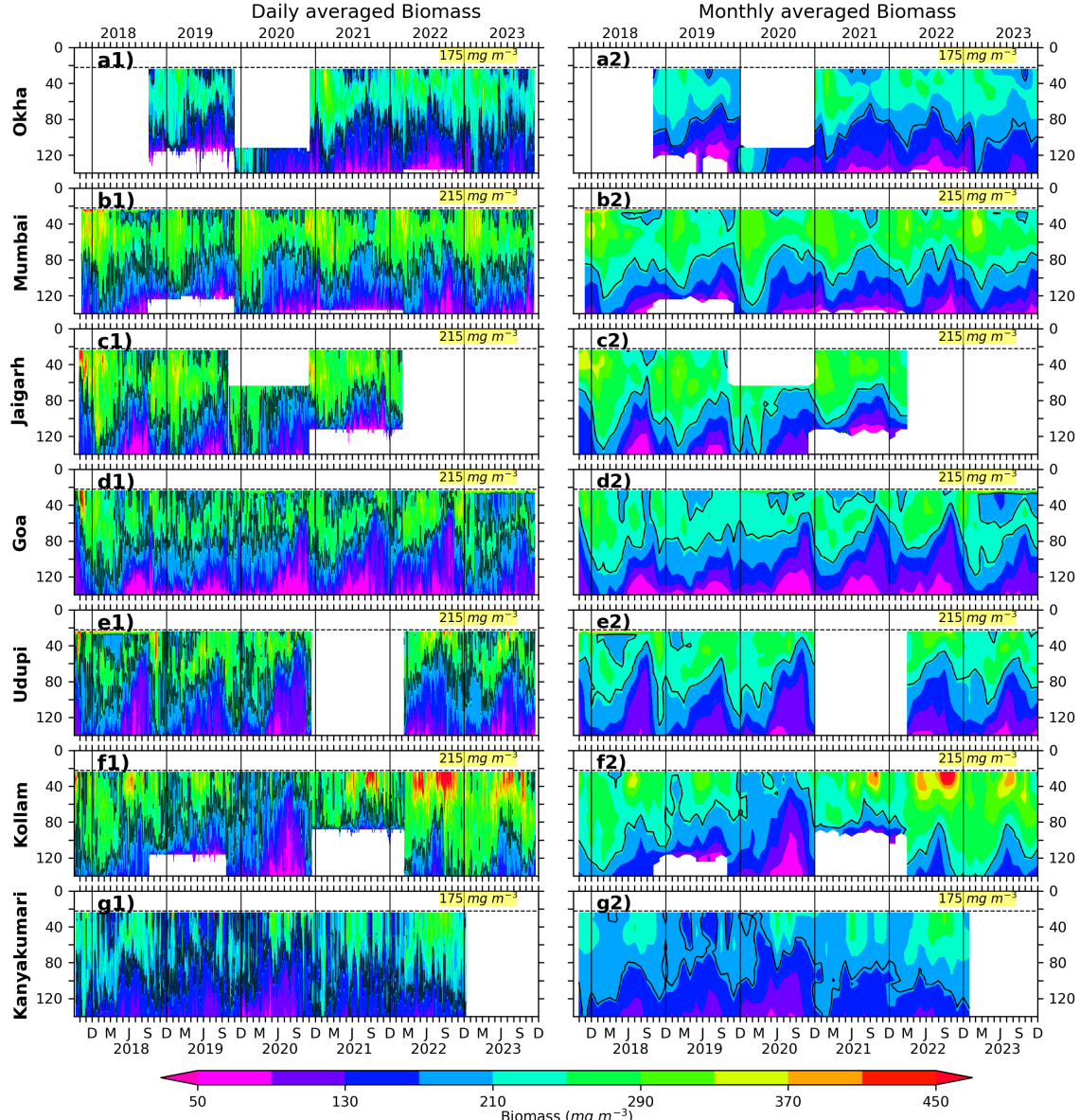


Figure 3: The Daily and monthly averaged biomass for EAS moorings, north (top) to south (bottom). The black contours are marking of 175 mg m^{-3} biomass for Okha and Kanyakumari; 215 mg m^{-3} for Mumbai, Goa and Kollam. The biomass contours are distinct and different based on the physico-chemical parameters and the one that best explains seasonality at respective location. The top 10 % of data is discarded due to echo noise. The dashed line at 22 m marks the top-depth of first bin i.e., 24 m.

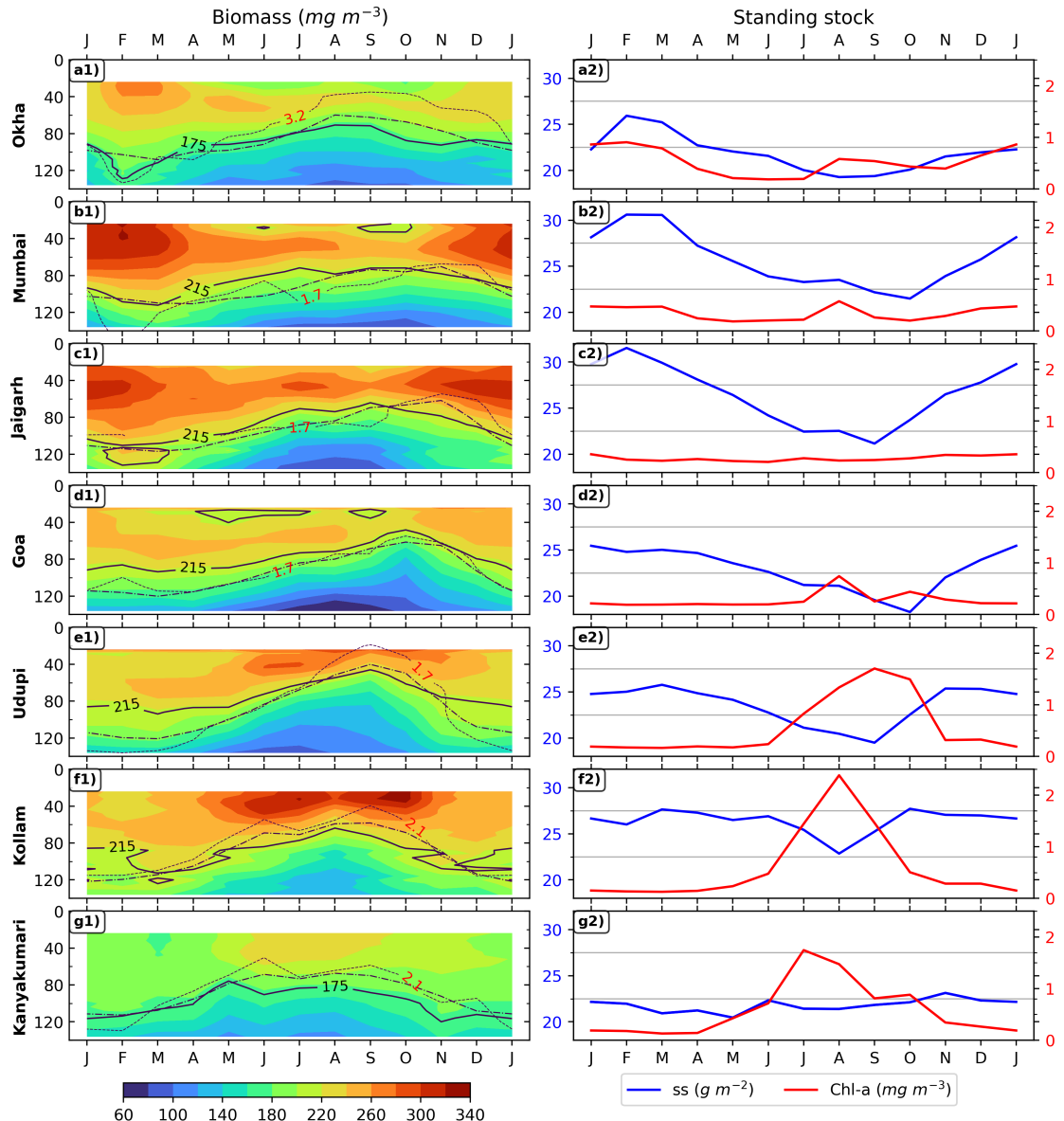


Figure 4: Monthly climatology of zooplankton biomass is shown in left panels for 7 locations, (top to bottom is southward). The D175 & D215 are shown in solid lines; dashed line represents the depth of 23 C isotherm; oxygen contours are shown in dotted lines and labeled for each mooring. The right set of panel plots is showing ZSS (24–140 biomass integral) and chlorophyll climatology for corresponding locations.

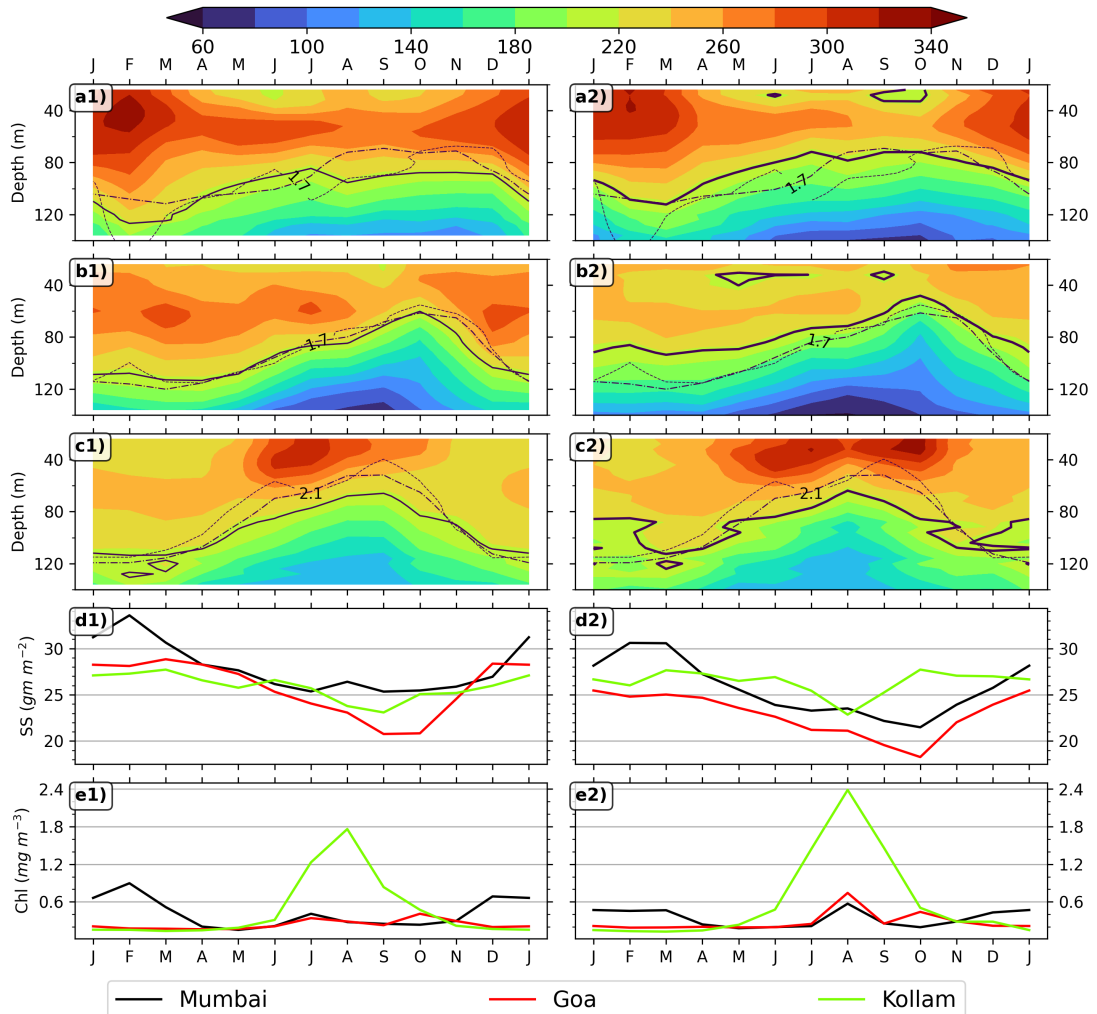


Figure 5: Monthly climatology of zooplankton biomass is shown in left panels for 3 locations which were earlier used in [Aparna et al., 2022]; a1, b1 & c1 is the biomass climatology for Mumbai, Goa and Kollam, d1 is for ZSS climatology (24–140 biomass integral), e1 is for chlorophyll biomass climatology; a2, b2, c2, d2 & e2 is same but based on data from 2017 to 2023. The D215 is shown in solid line. The dashed line represents the depth of 23 °C isotherm; oxygen contours are shown in dotted lines and labeled for each mooring.

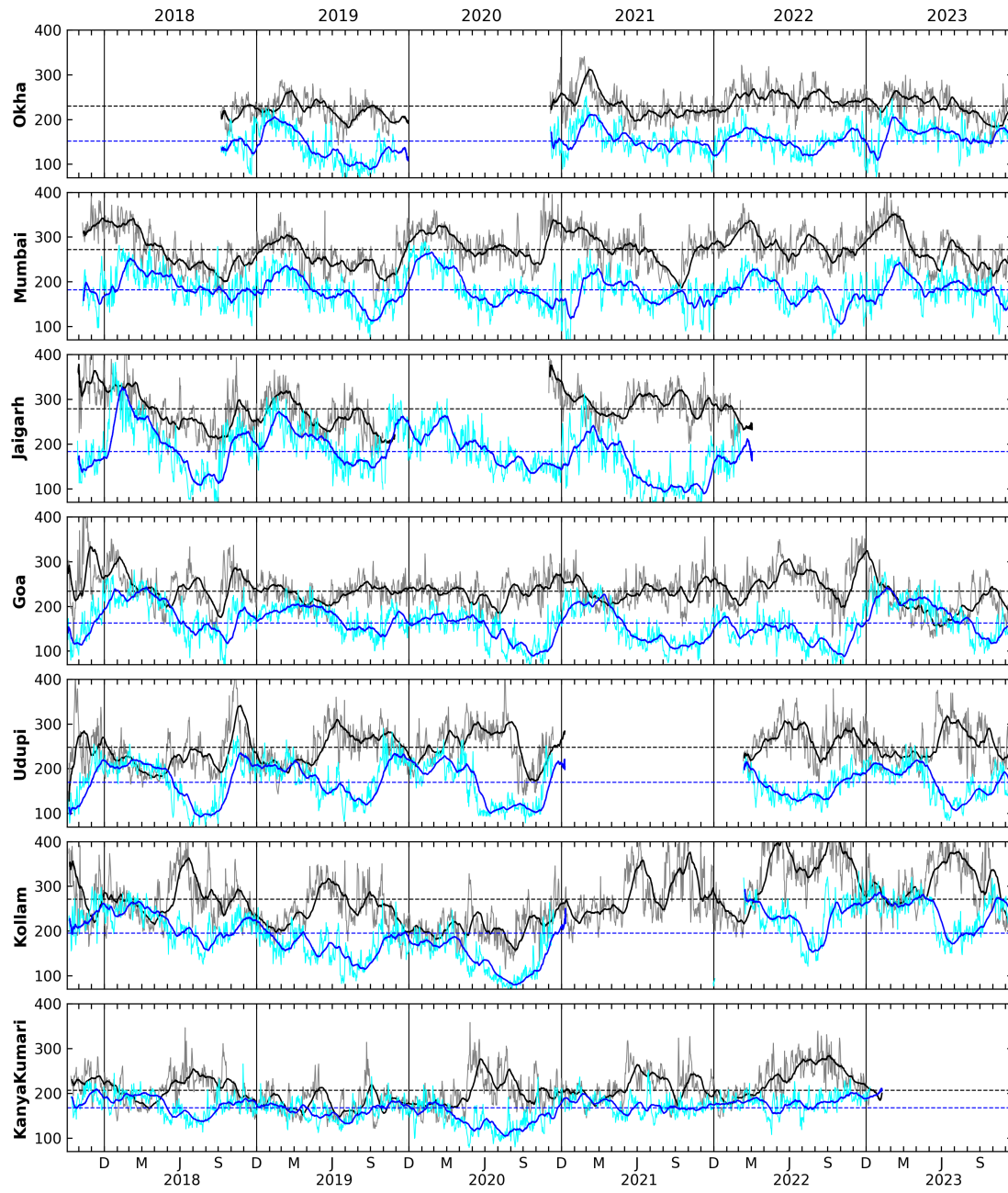


Figure 6: The daily biomass at depth of 40 m and 104 m for all locations shown by grey and cyan curves. The black and blue lines shows the 30 day rolling averaged biomass at 40 and 104 m, respectively. Notice the bursts seen in the daily data ranging from few days to weeks.

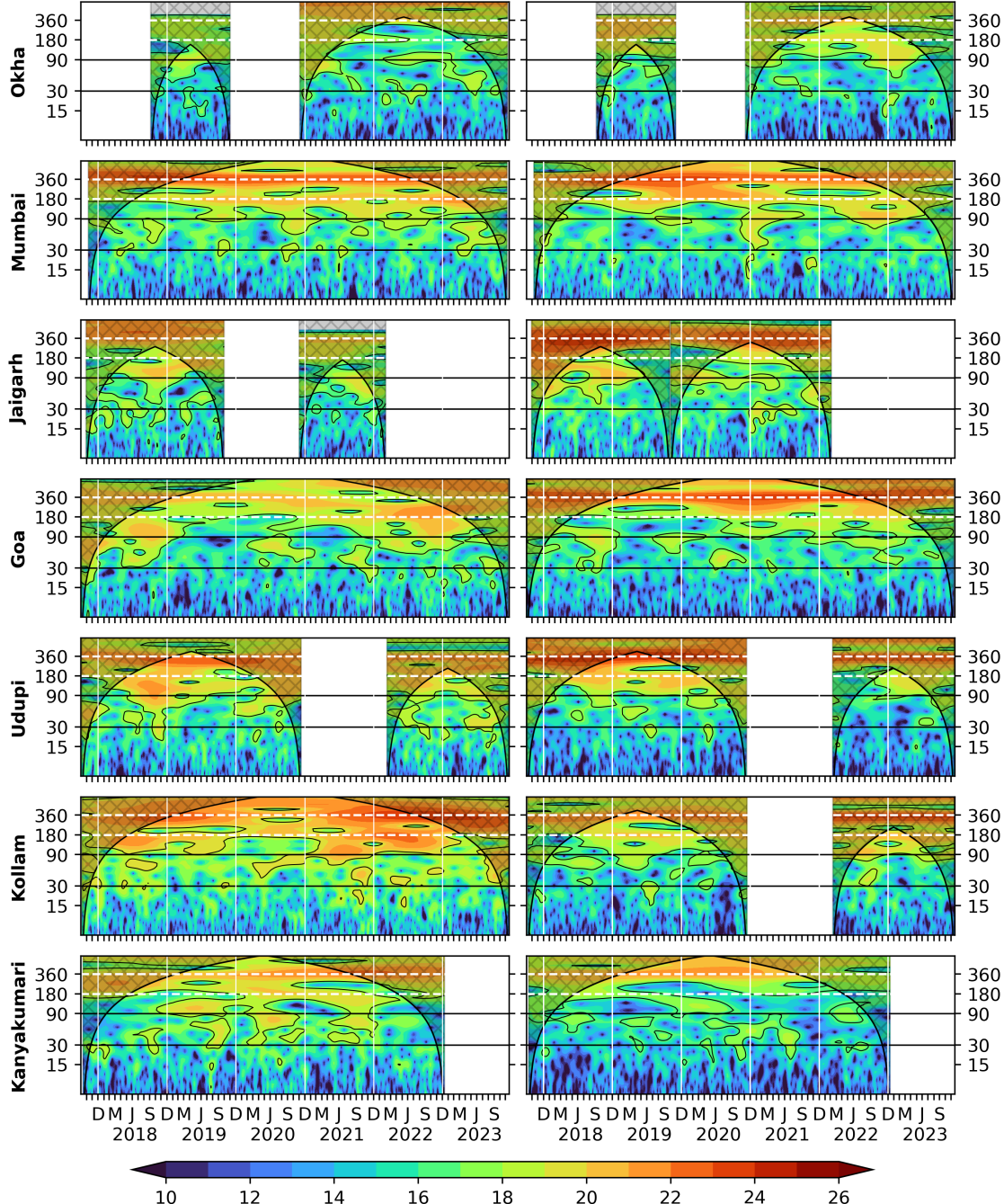


Figure 7: Wavelet power spectra (Morlet) of the 40 m (left panel) and 104 m (right panel) zooplankton biomass plotted against time as abscissa and period in days as ordinate. The wavelet power is in \log_2 scale, the 95 % significance is marked in black contours; the cross-shaded region falls under cone of influence. Vertical white lines separates years.

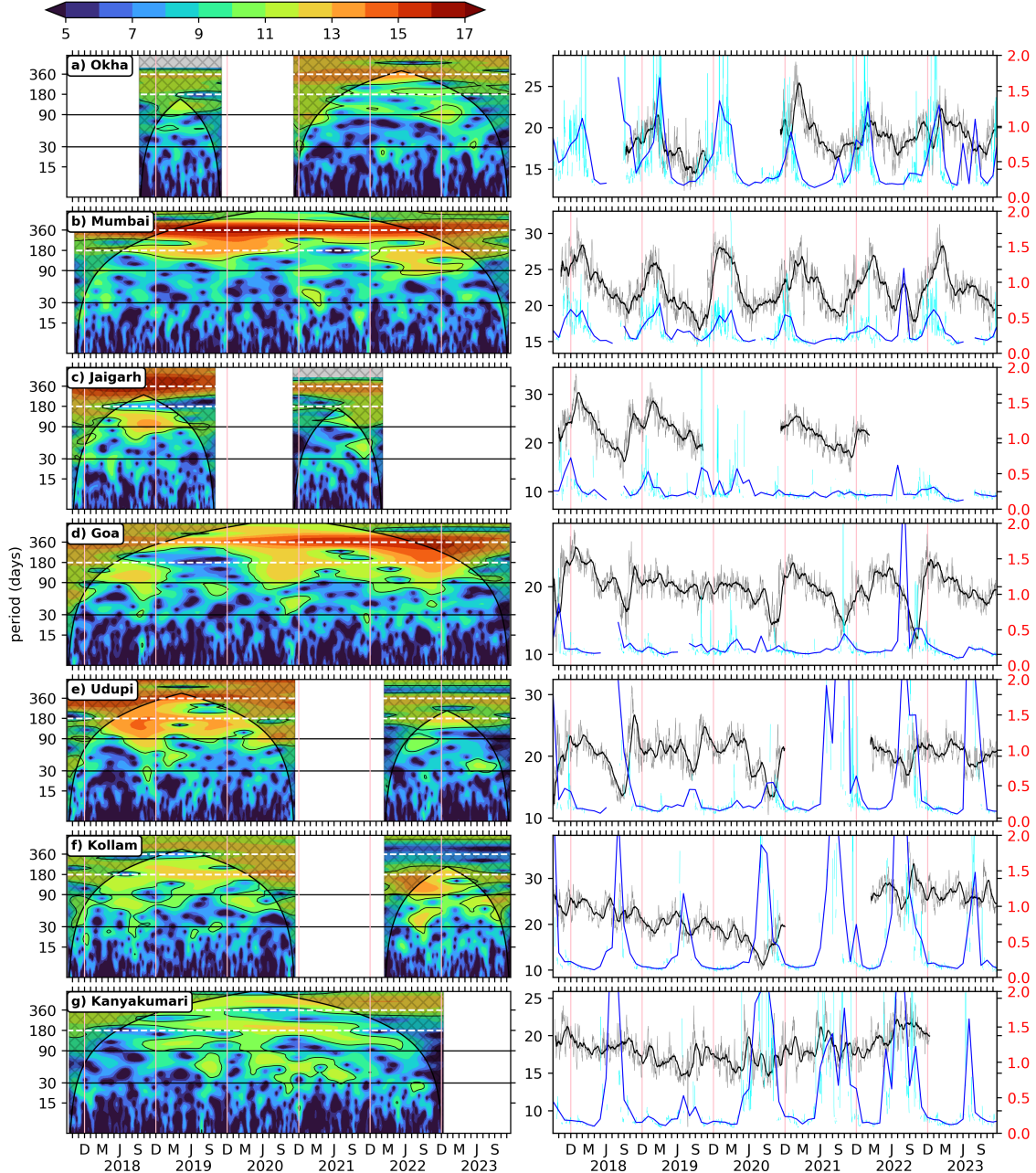


Figure 8: Wavelet power spectra (Morlet) of zooplankton standing stock plotted against time as abscissa and period in days as ordinate. The wavelet power is in log₂ scale, the 95 % significance is marked in black contours; The vertical white lines separates years. The right side panel shows the ZSS (24–120 m biomass integral) time series of 30 day rolling mean data (black) overlaid upon daily data (Grey). The 30 day rolling mean data of chlorophyll (solid blue) is plotted over its daily data (cyan).

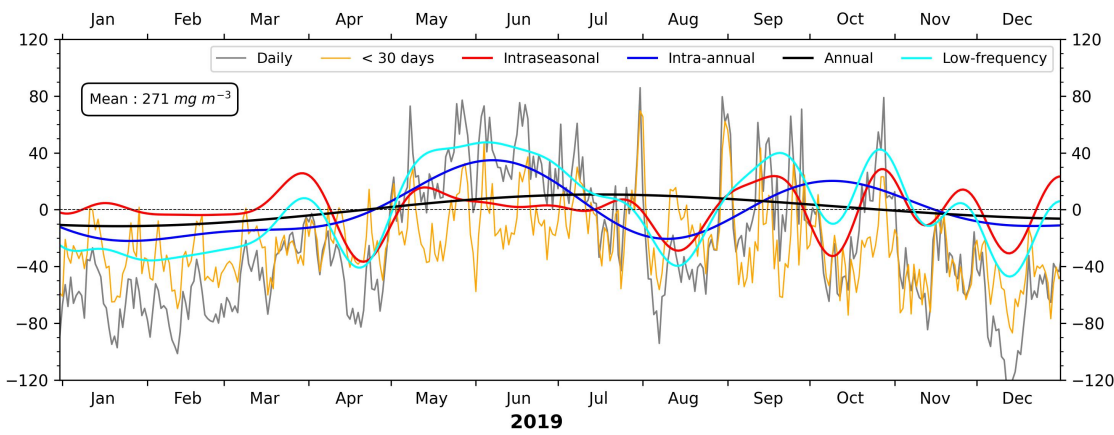


Figure 9: Comparison between mean-removed daily biomass time series at 40 m and the distinct components of variability off Kollam for 2019. The biomass units are mg m^{-3} . An increase in biomass is noticed from May onward and lasting till late monsoon with weeks of low biomass during August due to contribution from each component of variability. The cyan curve is sum of all low frequency components above 30 days, i.e, annual, intra-annual and 30 to 90 days intraseasonal variability.

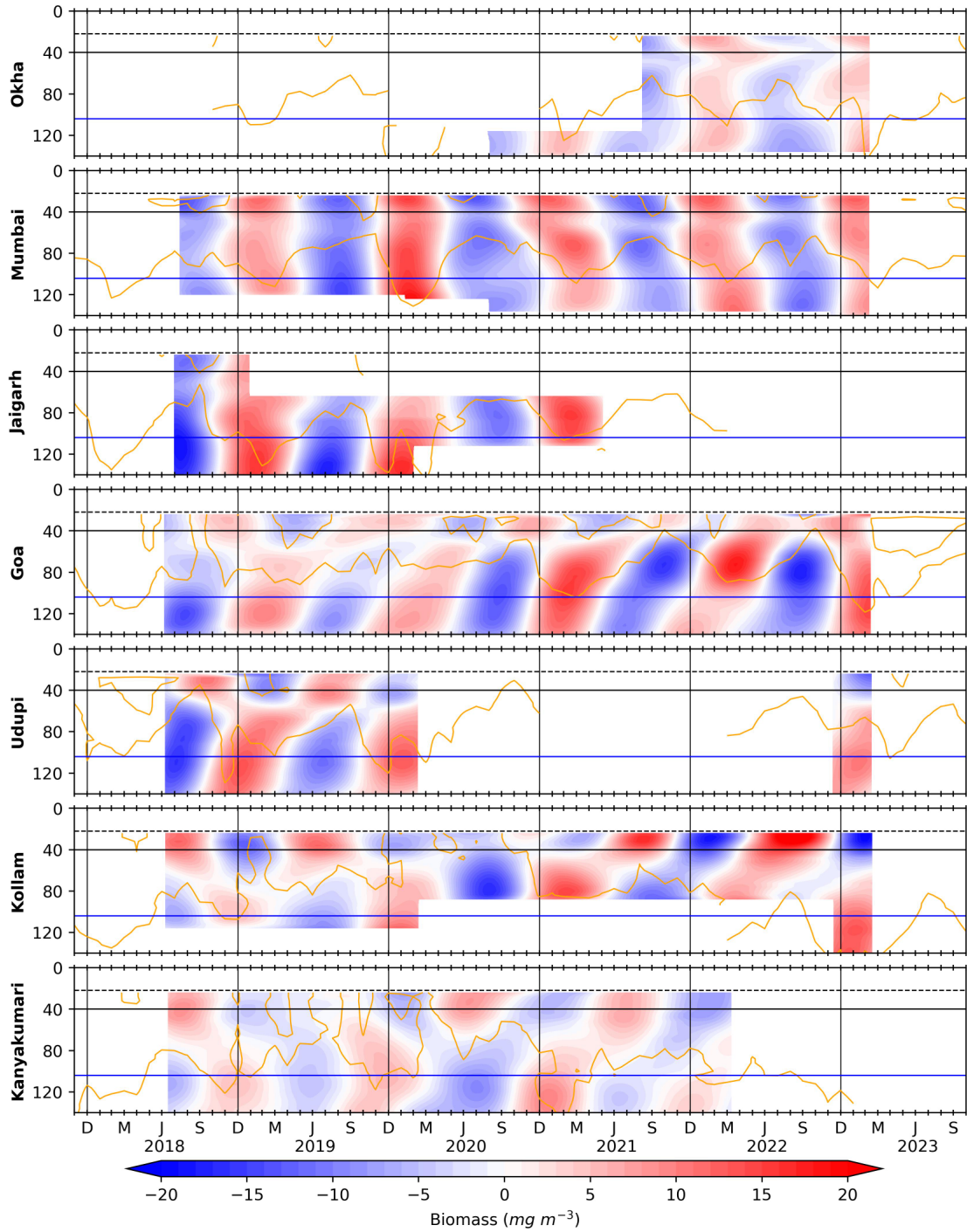


Figure 10: The biomass variation occurring in annual band (300 to 400 days). Owing to the presence of monsoon, there is a variation driven by associated upwelling (downwelling) processes in summer (winter) monsoon. and The horizontal black and blue lines is for 40 and 104 m respectively; vertical black lines separate the years. The dashed line at 22 m marks the top-depth of first bin i.e, 24 m ^{and} solid orange curves denotes D215 (D175 off Okha and Kanyakumari)

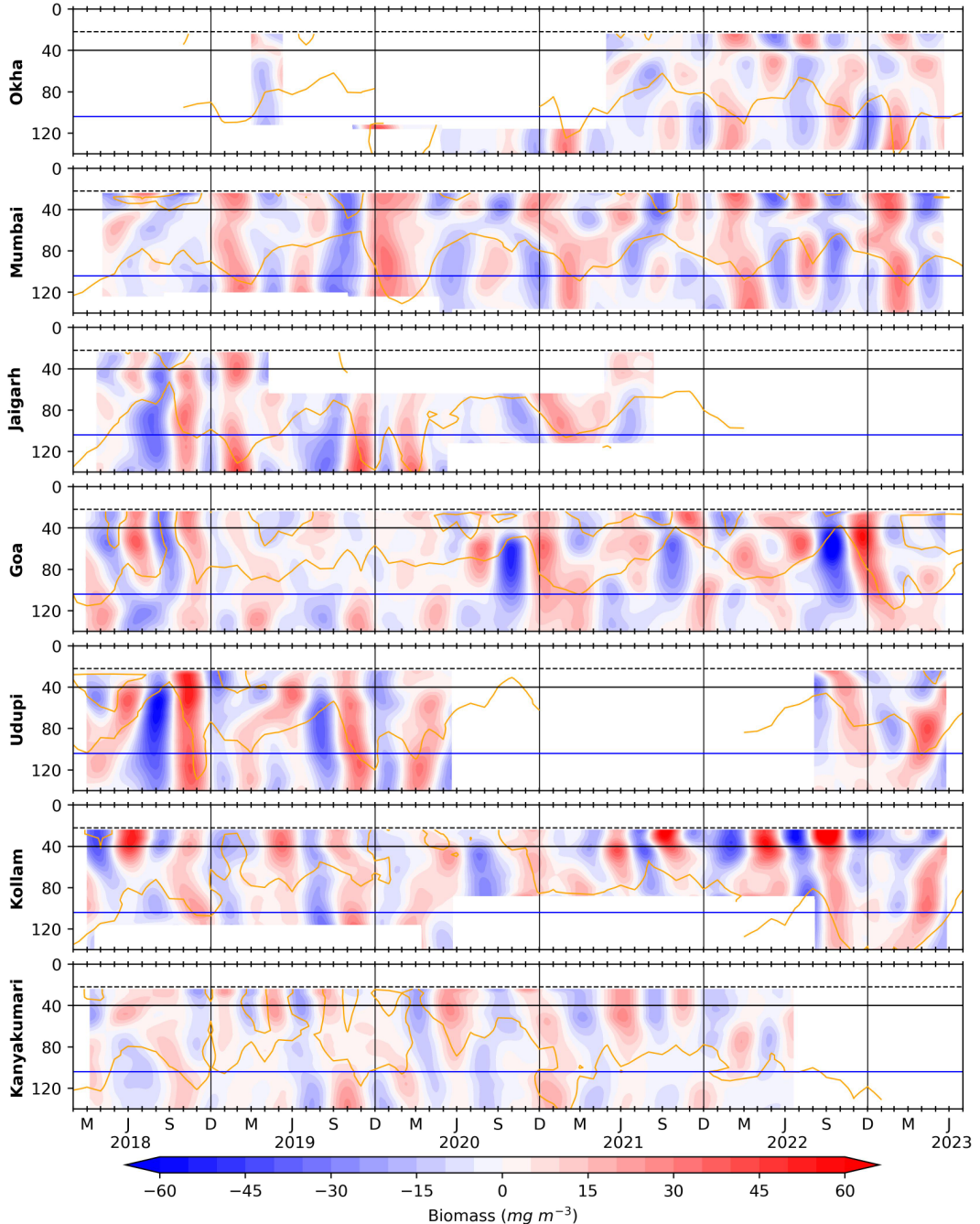


Figure 11: The biomass variation occurring in 100 to 250 days period (between the seasons and within a year record or intra-annual band) is obtained using a band pass filter. The horizontal black and blue lines is for 40 and 104 m respectively; vertical black lines separate the years. The dashed line at 22 m marks the top-depth of first bin i.e, 24 m and solid orange curves denotes D215 (D175 off Okha and Kanyakumari).

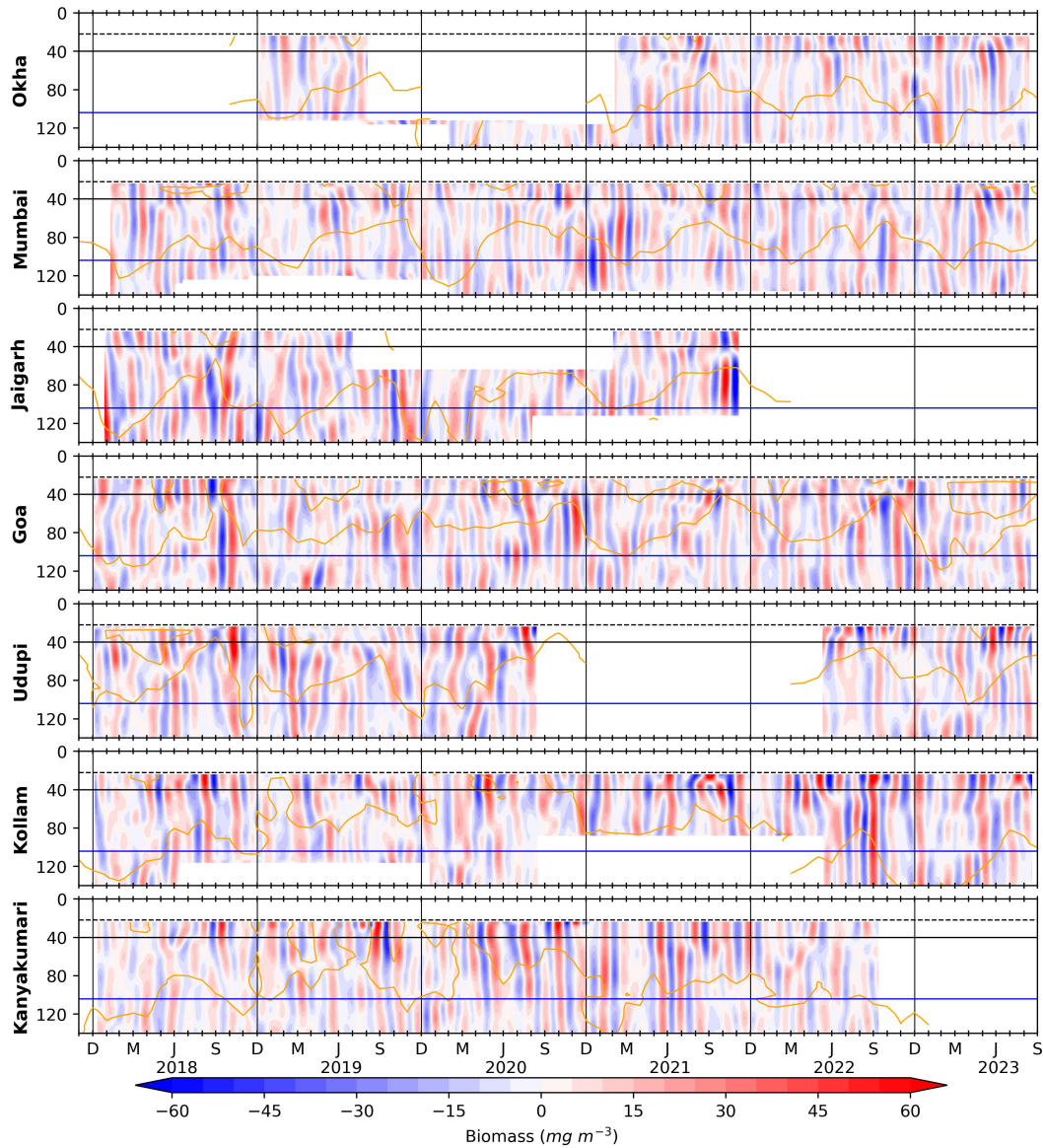


Figure 12: Biomass variation found in the scale of 30 to 90 days period (Intraseasonal band as it is within a season) is obtained using a lanczos band pass filter. The horizontal black and blue lines is for 40 and 104 m respectively; vertical black lines separate the years. The dashed line at 22 m marks the top-depth of first bin i.e, 24 m. Intraseasonal variability is seen throughout the record and the variability is stronger during August to November.

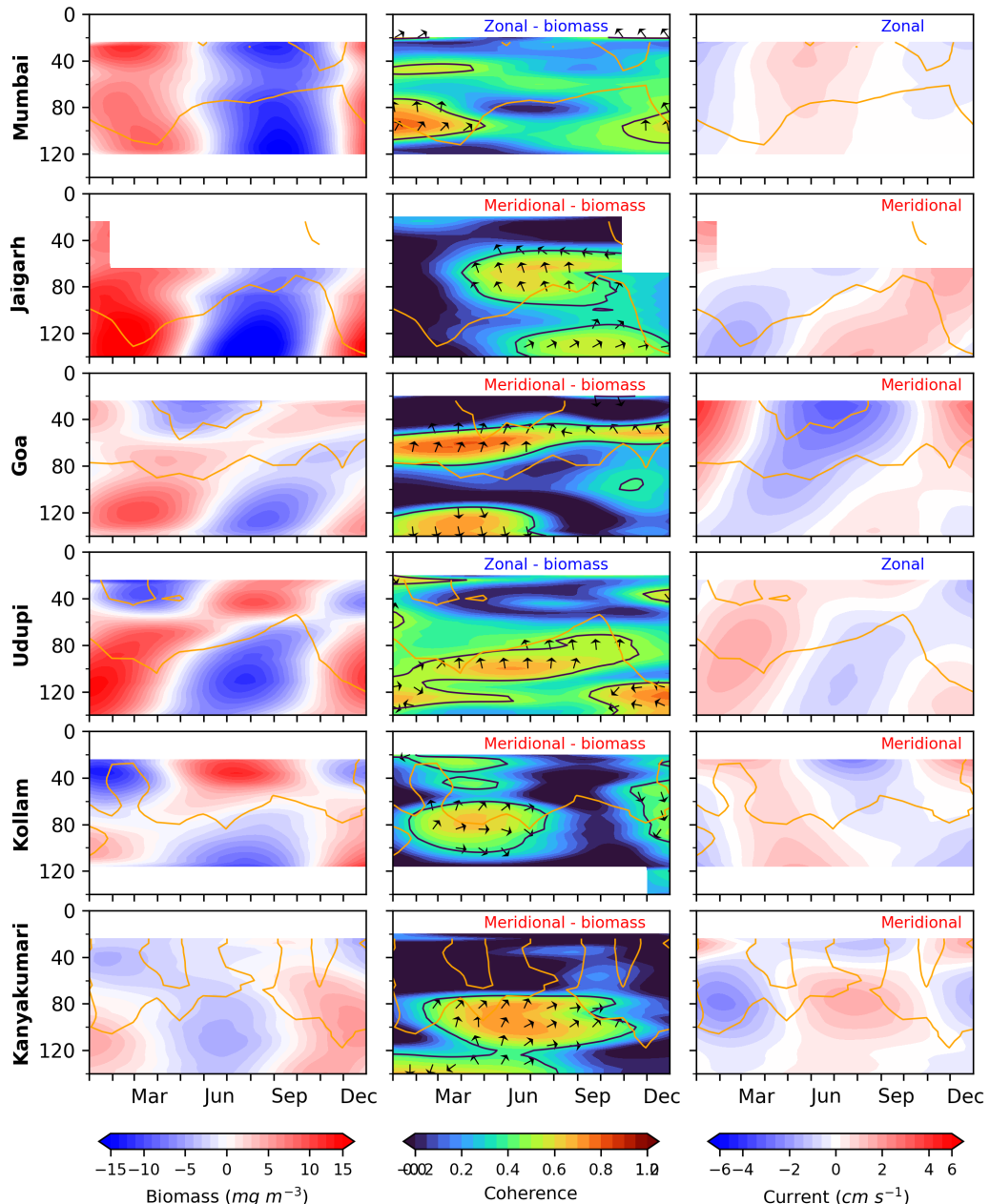


Figure 13: Current (zonal/meridional) and biomass wavelet coherence plotted alongside of annual filtered biomass and current. Either zonal or meridional current is considered depending on coherence and if current leads biomass. The solid contour encompasses greater than 0.5 coherence and phase is plotted with north as reference, +ve (-ve) x-axis is current leading (lagging) biomass. Left (Right) panel is for biomass (current). Although the annual biomass variability is weak and contributes less to the total biomass time series, upward phase propagation is seen implying upwelling favorable conditions leading to biomass growth. The solid orange curves denotes D215 (D175 off Okha and Kanyakumari)